the plant journal

SEB SOCIETY FOR EXPERIMENTAL BIOLOGY

The Plant Journal (2020) **103,** 660–676 doi: 10.1111/tpj.14759

AtMYB92 enhances fatty acid synthesis and suberin deposition in leaves of *Nicotiana benthamiana*

Alexandra To[1], Jérôme Joubès[2,3], Jean Thueux[1], Sami Kazaz[1,4], Loïc Lepiniec[1] and Sébastien Baud[1,*]

[1]*Institut Jean-Pierre Bourgin, INRAE, CNRS, AgroParisTech, Université Paris-Saclay, 78000 Versailles, France,*
[2]*Laboratoire de Biogenèse Membranaire, UMR 5200, Université de Bordeaux, 33882, Villenave d'Ornon, France,*
[3]*Laboratoire de Biogenèse Membranaire, UMR 5200, CNRS, 33882, Villenave d'Ornon, France, and*
[4]*Université Paris-Sud, Université Paris-Saclay, 91400, Orsay, France*

Received 23 September 2019; revised 2 February 2020; accepted 18 March 2020; published online 3 April 2020.
*For correspondence (e-mail sebastien.baud@inrae.fr).

SUMMARY

Acyl lipids are important constituents of the plant cell. Depending on the cell type, requirements in acyl lipids vary greatly, implying a tight regulation of fatty acid and lipid metabolism. The discovery of the WRINKLED1 (WRI1) transcription factors, members of the AP2-EREBP (APETALA2-ethylene-responsive element binding protein) family, has emphasized the importance of transcriptional regulation for adapting the rate of acyl chain production to cell requirements. Here, we describe the identification of another activator of the fatty acid biosynthetic pathway, the Arabidopsis MYB92 transcription factor. This MYB and all the members of the subgroups S10 and S24 of MYB transcription factors can directly activate the promoter of *BCCP2* that encodes a component of the fatty acid biosynthetic pathway. Two adjacent MYB *cis*-regulatory elements are essential for the binding and activation of the *BCCP2* promoter by MYB92. Overexpression of *MYB92* or *WRI1* in *Nicotiana benthamiana* induces the expression of fatty acid biosynthetic genes but results in the accumulation of different types of acyl lipids. In the presence of WRI1, triacylglycerol biosynthetic enzymes coded by constitutively expressed genes efficiently channel the excess fatty acids toward reserve lipid accumulation. By contrast, MYB92 activates both fatty acid and suberin biosynthetic genes; hence, the remarkable increase in suberin monomers measured in leaves expressing *MYB92*. These results provide additional insight into the molecular mechanisms that control the biosynthesis of an important cell wall-associated acylglycerol polymer playing critical roles in plants.

Keywords: MYB92, suberin, fatty acid, transcription factor, Arabidopsis, *Nicotiana benthamiana*.

INTRODUCTION

In plant cells, the biosynthesis of fatty acids (FAs) occurs in plastids (Harwood, 1996). The building block used for FA production, acetyl-CoA, is generated from end products of the glycolysis by the pyruvate dehydrogenase complex. Then, malonyl-CoA is formed from acetyl-CoA by heteromeric acetyl-CoA carboxylase (ACCase). The malonyl group of malonyl-CoA is subsequently transferred to an acyl carrier protein (ACP). Production of saturated acyl chains is catalyzed by the type II FA synthase, which uses acetyl-CoA as a starting unit, whereas the two-carbon units required for chain elongation are provided by malonyl-ACP. Thioesterases ultimately hydrolyze 16- or 18-carbon acyl chains, releasing FAs. Acyl lipids are derived from FAs and fulfill different roles in plant cells. As in other organisms, they are the basic structural components of the cell membranes (Mamode Cassim *et al.*, 2019). Triacylglycerols, triesters of FAs and glycerol, then represent a major form of carbon and energy storage in most oleaginous species (Baud, 2018). In addition, cuticular lipids (suberin, cutin, cuticular waxes) constitute lipophilic cell wall-associated barriers that prevent water loss, entry of pathogenic microorganisms and organ adherence (Kunst and Samuels, 2009; Delude *et al.*, 2016). Finally, a minor fraction of acyl lipids and their derivatives (e.g. jasmonate) participate in signaling pathways (Wasternack, 2007).

It was estimated that mesophyll cells contain 5–10% acyl lipids by dry weight, mostly in the form of membrane lipids (Ohlrogge and Browse, 1995). By contrast, in the seeds and in the fruit mesocarp of certain oleaginous species, cells can accumulate up to 90% triacylglycerols by dry weight (Bourgis *et al.*, 2011). The rate of acyl chain production thus varies considerably from one cell type to another, allowing the balancing of carbon supply and demand for

acyl chains to meet their specific requirements (Ohlrogge and Jaworski, 1997). The question of the nature of the molecular mechanisms underpinning the regulation of FA metabolism follows logically. Post-translational regulation targeting enzymes of the pathway such as heteromeric ACCase has been documented (Feria Bourrellier *et al.*, 2010; Andre *et al.*, 2012; Salie *et al.*, 2016). They allow subtle and rapid modifications of the rate of FA biosynthesis in response to varying environmental or physiological conditions (Salie and Thelen, 2016; Troncoso-Ponce *et al.*, 2016). Aside from such regulation, extensive transcriptomic analyses have revealed a strong correlation between transcript levels of genes encoding core FA biosynthetic enzymes and the rate of acyl chain production (Girke *et al.*, 2000; Troncoso-Ponce *et al.*, 2011). These studies have emphasized the key role played by transcriptional regulation in the developmental control of FA biosynthesis, particularly in oleaginous seeds and fruits. They have also outlined the coexpression cluster made of FA biosynthetic genes (Baud and Lepiniec, 2009; Peng and Weselake, 2011; Guerin *et al.*, 2016).

Arabidopsis thaliana WRINKLED1 (WRI1), the first transcriptional activator of FA biosynthesis identified in plants, is a member of the APETALA2-ethylene-responsive element binding protein (AP2-EREBP) family of transcription factors (TFs) (Cernac and Benning, 2004). Upon binding to AW *cis*-regulatory elements ($CnTnG[n]_7CG$) conserved among proximal upstream regions of several late glycolytic and FA biosynthetic genes (Maeo *et al.*, 2009), WRI1 recruits the Mediator complex and, in turn, the Pol II complex to initiate their transcription (Kim *et al.*, 2016). WRI1 TFs and AW *cis*-regulatory elements have been described in a range of plant species, where their function appears to be well conserved (Shen *et al.*, 2010; Marchive *et al.*, 2014). The genomes of land plants usually code for several related WRI1-like TFs that define a family of transcriptional regulators capable of triggering sustained rates of acyl chain synthesis. Contrasting expression patterns of the genes encoding these TFs usually contribute to specify their functions *in planta* (To *et al.*, 2012; Dussert *et al.*, 2013).

The observation that the Arabidopsis *wri1 wri3 wri4* triple knockout mutants maintain a basal level of FA biosynthetic gene expression suggests that the transcriptional machinery governing FA biosynthesis may include additional regulatory proteins. Furthermore, putative *cis*-regulatory elements distinct from the AW-box are overrepresented in the promoter regions of FA biosynthetic genes (Peng and Weselake, 2011) and some of these were shown to be essential for transcriptional activation of the corresponding genes (Baud *et al.*, 2009b). This further suggests that TFs not related to the WRIs and belonging to redundant regulatory pathways play a meaningful role in the transcriptional activation of FA biosynthesis. Besides, two members of the DNA-binding-with-one-finger (DOF) family of TFs have been proposed to activate the transcription of some FA biosynthetic genes in soybean (Wang *et al.*, 2007).

To isolate other regulators involved in the transcriptional regulation of the FA biosynthetic pathway, complementary screening procedures were undertaken. In the present study, we report the identification and functional characterization of the Arabidopsis MYB92 (At5g10280) TF and of close homologs of the MYB family. Yeast one-hybrid experiments and electrophoretic mobility shift assays show that MYB92 is able to interact with the promoter of *BIOTIN CARBOXYL CARRIER PROTEIN2* (*BCCP2*), a gene coding for a subunit of heteromeric ACCase. The binding of MYB92 to *ProBCCP2* requires two adjacent MYB *cis*-elements and is independent of the binding of WRI1 to the same promoter. It is then demonstrated that MYB92 activates *in planta* the *BCCP2* promoter, as well as other promoters of FA biosynthetic genes. By overexpressing *MYB92* in leaves of *Nicotiana benthamiana*, we further demonstrate its ability to enhance expression of not only FA, but also aliphatic suberin biosynthetic genes; hence, the remarkable deposition of suberin measured in this system.

RESULTS

Isolation of transcription factors binding *ProBCCP2*

A yeast one-hybrid screening procedure was implemented to isolate transcriptional regulators of the FA biosynthetic pathway. As bait, we employed a 180-bp DNA fragment located immediately upstream of the translational start codon of the Arabidopsis *BCCP2* gene, referred to as *ProBCCP2*. *BCCP2*, for which the expression profile is representative of FA biosynthetic genes (Baud and Lepiniec, 2009), codes for a subunit of heteromeric ACCase. Functional analyses previously established that the 180-bp DNA fragment used, which is part of the 5′-UTR of *BCCP2*, contained information required for the proper regulation of *BCCP2* expression *in planta* (Baud *et al.*, 2009b). The REGIA library, an ordered cDNA expression library for a set of Arabidopsis TFs (Paz-Arez, 2002), was screened by mating with a yeast strain containing the *ProBCCP2:HIS3* reporter construct. Among the 926 open reading frames of the library, two candidates were isolated. As reported previously, one of the candidates encoded WRI3, a member of the AP2-EREBP family (To *et al.*, 2012). The second encoded MYB92, the function of which was investigated further.

MYB92 interacts with *ProBCCP2* through adjacent MYB elements

Confirmation of the interaction between MYB92 and the *BCCP2* promoter was first performed using a yeast one-

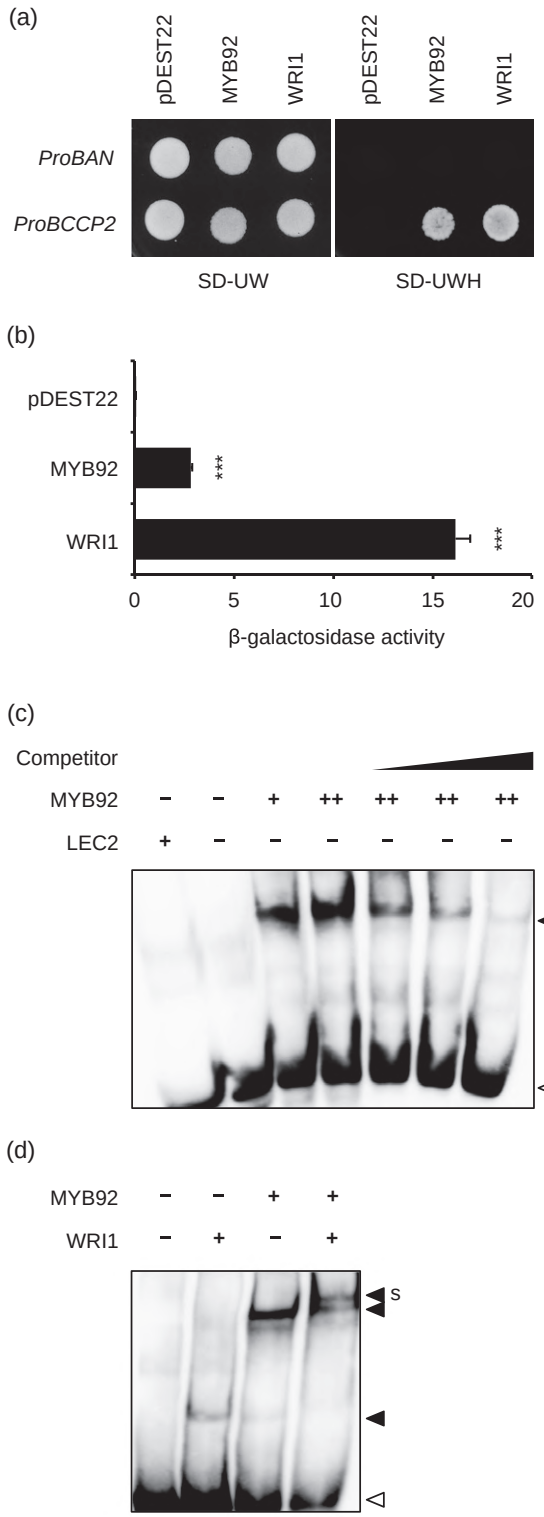

Figure 1. Interaction of MYB92 with the promoter of the *BCCP2* gene. (a) Analysis of MYB92 binding to the promoter of *BCCP2* in yeast one-hybrid experiments. Yeast strains containing the *HIS3* reporter gene under the control of either the *BANYULS* (*BAN*, negative control) or *BCCP2* promoter were transformed with either the empty pDEST22 expression vector or with a version of this vector allowing the expression of MYB92 or WRI1 before being plated on appropriate media to maintain the expression of the vectors (SD-UW) and to test the activation of the *HIS3* reporter gene (SD-UWH). The data presented are representative of the results obtained for five independent colonies. SD, synthetic drop-out medium. (b) Quantification of MYB92 binding to the promoter of *BCCP2* in yeast one-hybrid experiments. Yeast strains containing the *LacZ* reporter gene under the control of the *BCCP2* promoter were transformed with either the empty pDEST22 expression vector or with a version of this vector allowing the expression of MYB92 or WRI1 before being plated on appropriate media to maintain the expression of the vectors. ß-galactosidase activity was then measured to test the activation of the *LacZ* reporter gene. Values are the mean ± SE of 15 measurements carried out on five independent colonies. Asterisks indicate significant difference from the control according to a *t*-test (***$P < 0.001$). (c) Binding of MYB92 to the proximal upstream region of *BCCP2*. Electrophoretic mobility shift assay (EMSA) of a probe covering a region from −188 to −110 bp upstream from the ATG codon of *BCCP2* with increasing amounts of MYB92 ('+' = 0.4 μg, '++' = 0.8 μg). LEC2 was used as a negative control. Competition of MYB92 binding was carried out in the presence of 10-, 20- and 100-fold amounts of the unlabeled *ProBCCP2* fragment. Position of free probe (open arrowhead) and the shifted bands (closed arrowheads) are indicated. (d) Concomitant binding of MYB92 and WRI1 to the proximal upstream region of *BCCP2*. EMSA was carried in the same conditions as set out above. s, supershifted band.

hybrid approach. Yeast strains that presented the *HIS3* reporter gene under the control of a *BANYULS* (*BAN*, used as a negative control) or *BCCP2* promoter were constructed and transformed with different plasmids allowing the expression of MYB92 or WRI1 (positive control) as GAL4 activating domain (AD) fusions. A transformation of the strain presenting the *HIS3* reporter gene under the control of *BAN* promoter gave no positive interaction results, showing that MYB92 and WRI1 were unable to interact with this promoter (Figure 1a). By contrast, the expression of MYB92 or WRI1 in the strain presenting the *HIS3* reporter gene under the control of the *BCCP2* promoter resulted in the specific growth of the strain on medium lacking histidine, demonstrating the interaction between the TFs and this promoter sequence. To compare the strength of these interactions, quantitative ß-galactosidase assays were performed in yeast containing the *lacZ* reporter gene cloned downstream of *ProBCCP2*. Both MYB92 and WRI1 could activate the reporter gene and the reporter activity measured in the presence of WRI1 was higher (Figure 1b).

The binding of MYB92 to the *BCCP2* promoter sequence was further examined *in vitro* by electrophoretic mobility shift assay (EMSA). Purified recombinant MYB92 was produced and incubated with a 79-bp DNA fragment from the *BCCP2* promoter containing three putative MYB-core *cis*-elements (according to AthaMap; Steffens *et al.*, 2004) plus an AW-box (Maeo *et al.*, 2009) (Figure 2a). Binding was determined using biotin-labeled DNA probes. The addition of MYB92 to the DNA fragment yielded gel retardation (Figure 1c). The signal intensity increased with the concentration of the protein in the assay. The binding appeared to be specific because the addition of recombinant LEAFY COTYLEDON2 (LEC2) used as a negative control did not

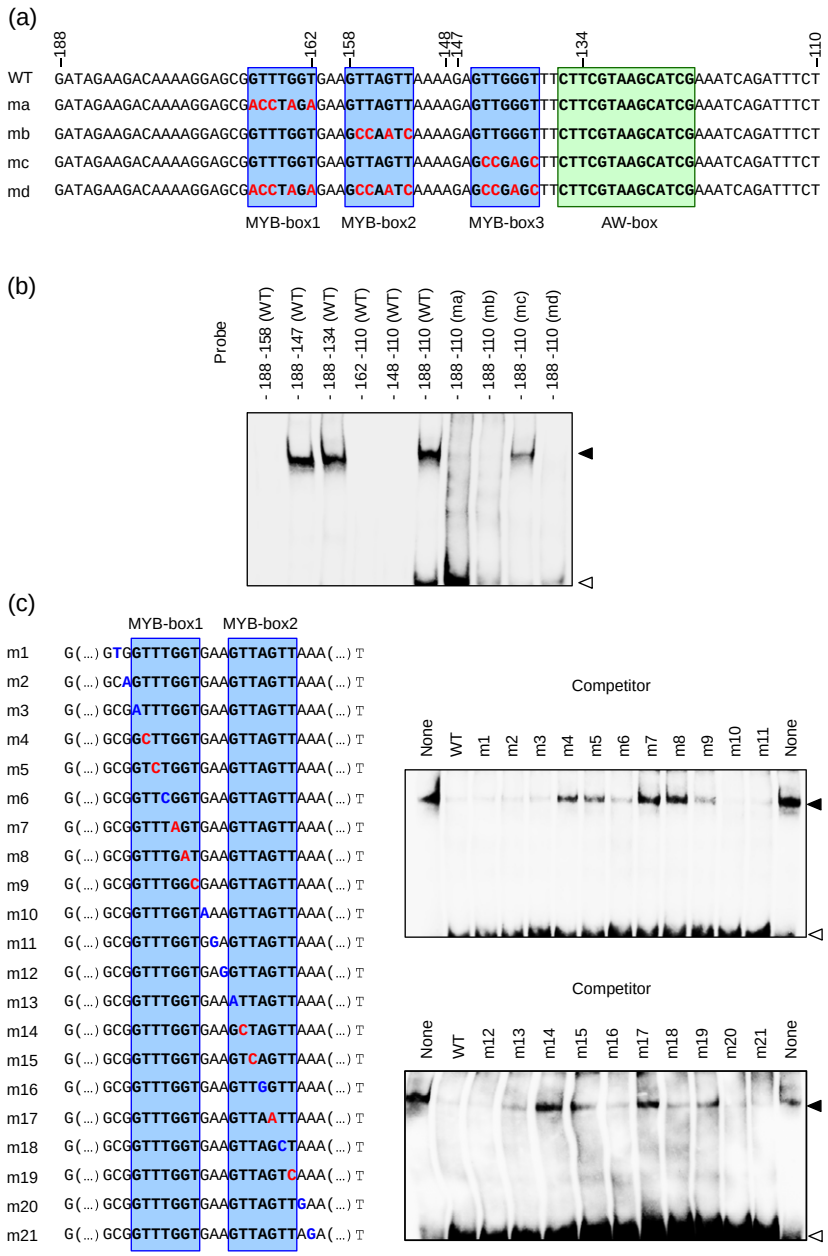

Figure 2. Interaction of MYB92 with two adjacent MYB *cis*-regulatory elements in the promoter of *BCCP2*. (a) Representation of the wild-type DNA probe covering a 79-bp region of the promoter of *BCCP2* (from −188 to −110 bp upstream from the ATG codon) and of mutagenized versions of this DNA probe used for electrophoretic mobility shift assay (EMSA). Positions of the AW (green box) and MYB *cis*-regulatory elements identified (blue boxes) are presented. Mutations are indicated in red. (b) Identification of the binding sites of MYB92 in the proximal upstream region of *BCCP2*. The EMSA of truncated and partially overlapping wild-type sequences (WT; lanes 1–5) and of mutagenized versions of the full-length probe (lanes 7–10) is presented. Position of free probe (open arrowhead) and the shifted bands (closed arrowheads) are indicated. (c) Binding site sequence specificity of MYB92. A competition of MYB92 binding to *ProBCCP2* (−188 to −110 bp) probe was carried out in the presence of unlabeled *ProBCCP2* fragments containing single mutations near the MYB elements 1 and 2. Mutations that affected MYB92 binding are indicated in red, whereas mutations that did not affect MYB92 binding are indicated in blue. The position of free probe (open arrowhead) and the shifted bands (closed arrowheads) are indicated. WT, wild-type.

result in the apparition of shifted bands. This specificity was confirmed by competition experiments with increasing amounts of unlabeled oligonucleotides that suppressed the binding of MYB92 to the labeled probe. The addition of WRI1 also led the formation of a shifted band of lower molecular weight (Figure 1d). The supershifted band observed upon addition of both MYB92 and WRI1 suggested that the two TFs could bind simultaneously to the *BCCP2* promoter (Figure 1d).

The 79-bp *BCCP2* promoter fragment used for EMSA was divided into five partially overlapping fragments containing one to three of the putative MYB-core *cis*-element each. MYB92 was able to bind only the fragments harboring both MYB elements 1 and 2 (Figure 2b). By means of nucleotide substitutions targeting one or several MYB-core *cis*-elements, mutagenized versions of the 79-bp *BCCP2* promoter sequence were then prepared. Mutations of the MYB boxes 1 or 2 impaired MYB92 binding, whereas the TF was still able to bind the *BCCP2* promoter containing a mutagenized version of MYB box 3 (Figure 2b). To precisely examine the specificity of the MYB92 binding sequence, we prepared various mutant forms of the sites surrounding the MYB-core elements 1 and 2 with single-base substitutions. Considering the high number of promoter versions to be assayed in this experiment, we decided to test them as unlabeled oligonucleotides in a

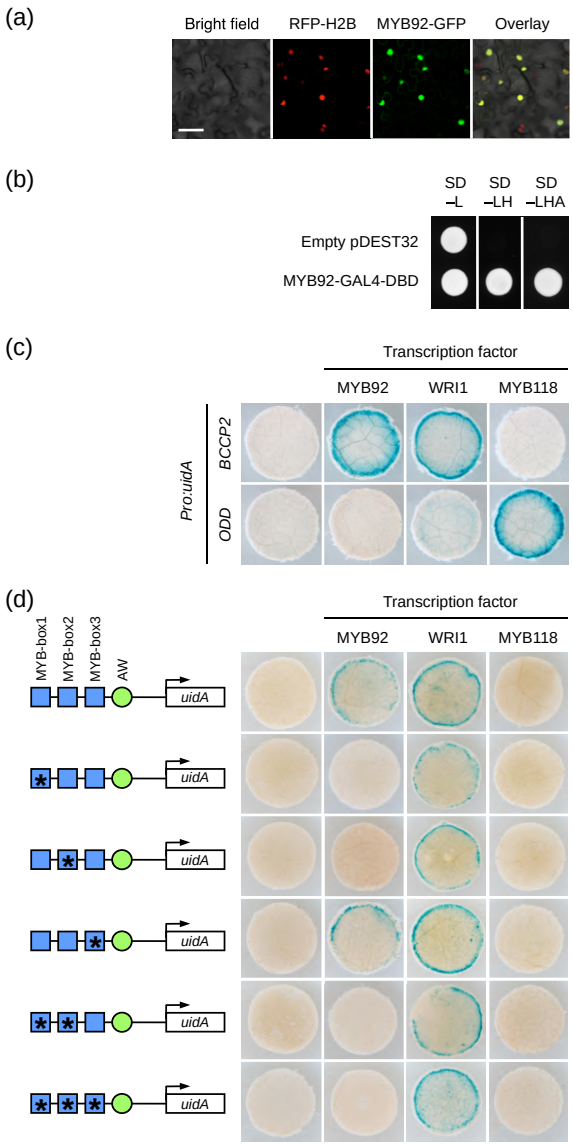

Figure 3. Transcriptional activation of the *BCCP2* promoter by MYB92. (a) Confocal micrographs showing localization of MYB92:GFP fusion proteins in *Nicotiana benthamiana* plants stably transformed with a construct coding for RFP:H2B fusion proteins (Martin *et al.*, 2009). Plants were co-infiltrated with the *Pro35Sdual:MYB92:GFP* construct and a vector encoding the p19 protein of tomato bushy stunt virus (TBSV) that prevents the onset of post-transcriptional gene silencing (Shamloul *et al.*, 2014). GFP was observed 4 days after infiltration. Scale bar = 50 μm. (b) Transcriptional activity of MYB92. MYB92 coding sequence was cloned in frame with the GAL4 DNA-binding domain (DBD). The fusion construct was introduced into reporter yeast containing the *HIS3* and *ADE2* reporter genes before being plated on appropriate media to maintain the expression of the vectors (SD-L) and to test the activation of the *HIS3* (SD-LH) or *HIS3* and *ADE2* reporter genes (SD-LHA). The data presented are representative of the results obtained for six independent colonies. SD, synthetic drop-out medium. (c) Transactivation assay in leaves of *Nicotiana benthamiana*. *Pro:uidA* reporter constructs alone or in combination with a vector allowing the expression of *MYB92*, *WRI1* or *MYB118* (negative control) were co-infiltrated in young leaves of *N. benthamiana* with a vector coding for the p19 protein. Leaf discs were assayed for GUS activity 4 days after infiltration. Tissues were incubated for 4.5 h in a buffer containing potassium ferrocyanide and potassium ferricyanide (each 2 mM). Representative discs (diameter 0.8 cm) are presented. (d) Transactivation assay in leaves of *Nicotiana benthamiana* with reporter constructs comprising mutagenized versions of the *BCCP2* promoter. Schematic representations of the reporter constructs used are presented. Blue squares and green circles denote wild-type *cis*-regulatory elements, and asterisks indicate that the MYB-core element was modified as follows: GTTTGGT → GCCTAGC (MYB-box 1), GTTAGTT → GCCATTC (MYB-box 2) and GTTGGGT → GCCATTC (Myb-box 3). Leaf discs harvested for GUS activity 4 days after infiltration were incubated for 2.5 h in a buffer containing potassium ferrocyanide and potassium ferricyanide (each 2 mM). Representative discs (diameter 0.8 cm) are presented.

competition assay. Mutations in five out of the seven nucleotides composing the MYB element 1 and in four out of the seven nucleotides composing the MYB element 2 resulted in a loss of MYB92 binding, whereas mutations outside of the motif showed no effect on MYB92 binding (Figure 2c). Altogether, these results established the importance of two adjacent MYB-core elements in the promoter sequence of *BCCP2* for MYB92 binding.

MYB92 is a transcriptional regulator able to activate expression of the *uidA* reporter gene cloned downstream of *ProBCCP2*

To demonstrate that MYB92 is a functional TF, we first investigated the *in vivo* subcellular localization of the protein with mGFP6, a derivative of green fluorescent protein (GFP). This derivative was fused to *MYB92* cDNA and placed under the control of the CaMV dual35S promoter for high and ubiquitous expression. The resulting construct was transfected into leaves of *N. benthamiana* stably transformed with a cassette coding for red fluorescent protein (RFP) fused to histone 2B, used as a nuclear marker (Martin *et al.*, 2009). Confocal imaging of transfected cells showed a co-localization of the GFP and RFP signals, establishing the nuclear targeting of the MYB92-GFP fusion (Figure 3a).

To determine whether MYB92 possesses transcriptional activity, the coding region of the TF was cloned in frame with the GAL4 DNA-binding domain (DBD). The construct obtained was introduced into a yeast strain (AH109) carrying the *ADE2* and *HIS3* reporter genes under the control of heterologous GAL4-responsive upstream activating sequences and promoter elements. The expression of the two reporters could be activated in the presence of MYB92 fused to GAL4-DBD, thus establishing the transcriptional activity of the TF (Figure 3b).

To test the ability of MYB92 to directly activate *ProBCCP2*, we used a *ProBCCP2:uidA* reporter construct in transactivation assays in *N. benthamiana*. The promoter of the *2-OXOGLUTARATE-DEPENDENT DIOXYGENASE* (*ODD*) gene cloned upstream of the *uidA* reporter gene was used as a negative control. Reporter constructs were infiltrated alone or in combination with a vector allowing the expression of *MYB92*, *WRI1* (positive control; Baud

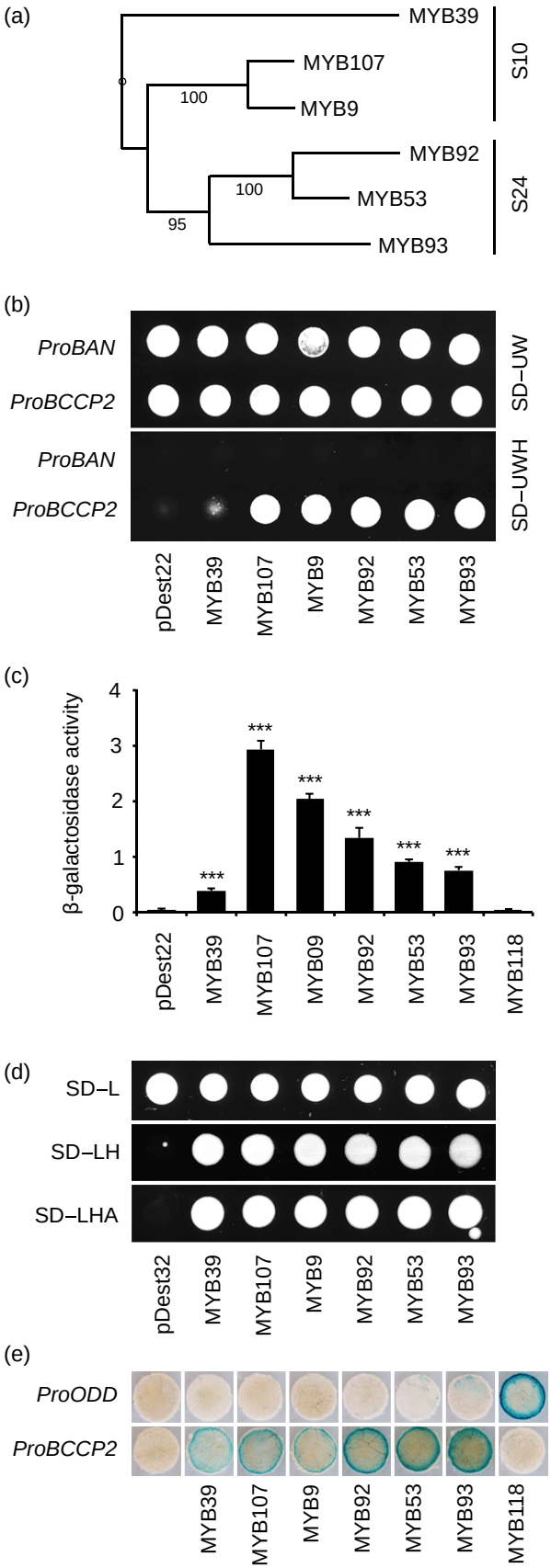

Figure 4. Activation of the *BCCP2* promoter by the MYB transcription factors comprising subgroups S10 and S24. (a) Phylogram, with branch lengths in arbitrary units, using the alignment generated by MAFFT. Full-length sequences of the MYB transcription factors (with gaps) were used for the distance analyses. (b) Analysis of MYB binding to the promoter of *BCCP2* in yeast one-hybrid experiments. Yeast strains containing the *HIS3* reporter gene under the control of either the *BANYULS* (*BAN*, negative control) or *BCCP2* promoter were transformed with either the empty pDEST22 expression vector or with a version of this vector allowing the expression of the MYBs before being plated on appropriate media to maintain the expression of the vectors (SD-UW) and to test the activation of the *HIS3* reporter gene (SD-UWH). The data presented are representative of the results obtained for five independent colonies. SD, synthetic drop-out medium. (c) Quantification of MYB binding to the promoter of *BCCP2* in yeast one-hybrid experiments. Yeast strains containing the *LacZ* reporter gene under the control of the *BCCP2* promoter were transformed with either the empty pDEST22 expression vector or with a version of this vector allowing the expression of the MYBs before being plated on appropriate media to maintain the expression of the vectors. ß-galactosidase activity was then measured to test the activation of the *LacZ* reporter gene. Values are the mean ± SE of 18 measurements carried out on six independent colonies. Asterisks indicate a significant difference from the control according to a *t*-test (***$P < 0.001$). (d) Transcriptional activity of the MYB transcription factors. *MYB* coding sequences were cloned in frame with the GAL4 DNA-binding domain (DBD). The fusion constructs were introduced into reporter yeast containing the *HIS3* and *ADE2* reporter genes before being plated on appropriate media to maintain the expression of the vectors (SD-L) and to test the activation of the *HIS3* (SD-LH) or *HIS3* and *ADE2* reporter genes (SD-LHA). The data presented are representative of the results obtained for six independent colonies. (e) Transactivation assay in leaves of *Nicotiana benthamiana*. *Pro:uidA* reporter constructs alone or in combination with a vector allowing the expression of the *MYBs* were co-infiltrated in young leaves of *N. benthamiana* with a vector coding for the p19 protein. Leaf discs were assayed for GUS activity 4 days after infiltration. Tissues were incubated 3 h in a buffer containing potassium ferrocyanide and potassium ferricyanide (each 2 mM). Representative discs (diameter 0.8 cm) are presented.

et al., 2009b) or *MYB118* (negative control; Barthole *et al.*, 2014) in young leaves of *N. benthamiana*. MYB92, similar to WRI1, was able to activate the *ProBCCP2:uidA* reporter construct, showing a strong increase in GUS activity compared to the reporter alone (Figure 3c).

Transient activation assays were repeated with mutagenized versions of the *BCCP2* promoter (Figure 3d). Mutations in the MYB-core *cis*-elements did not affect the ability of WRI1 to activate the promoter. By contrast, MYB92 was no longer able to activate mutagenized versions of the *BCCP2* promoter comprising a mutagenized version of MYB box 1 or 2, confirming the importance of these two adjacent *cis*-regulatory elements for transcriptional activation of *ProBCCP2* by the MYB TF.

All members of the subgroups S10 and S24 of MYB transcription factors activate *ProBCCP2:uidA* in transactivation assays

MYB92 belongs to subgroup S24 of MYB TFs (Dubos *et al.*, 2010) (Figure 4a). Because several members of this and related S10 subgroups were absent from the REGIA library, the six full-length cDNAs (*MYB93*, *MYB92*, *MYB53*, *MYB39*, *MYB107* and *MYB9*) were systematically cloned in the pDEST22 vector allowing expression of GAL4-AD-MYB

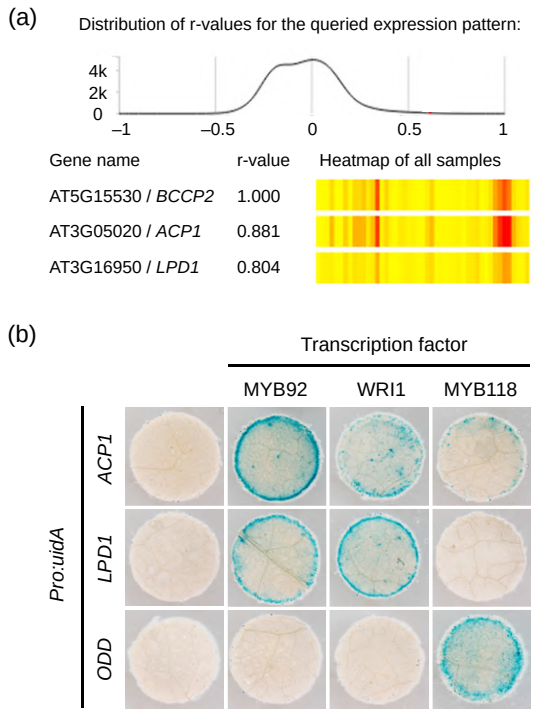

Figure 5. Activation of the promoters of fatty acid biosynthetic genes by MYB92. (a) Genes coexpressed with *MYB92* in Arabidopsis. Output of a query on Expression Angler 2016 (developmental map; with default values) displaying an eFP image depicting the expression data and correlation coefficients for the two genes exhibiting the most similar expression patterns with *MYB92*. (b) Transactivation assay in leaves of *Nicotiana benthamiana*. *Pro:uidA* reporter constructs alone or in combination with a vector allowing the expression of *MYB92*, *WRI1* or *MYB118* (negative control) were co-infiltrated in young leaves of *N. benthamiana* with a vector coding for the p19 protein. Leaf discs were assayed for GUS activity 4 days after infiltration. Tissues were incubated 2 h in a buffer containing 2 mM each of potassium ferrocyanide and potassium ferricyanide. Representative discs (diameter 0.8 cm) are presented.

fusion proteins in yeast cells carrying the *HIS3* reporter gene under the control of the *BCCP2* promoter. The corresponding fusion proteins were all able to induce yeast growth on selective medium, demonstrating their interaction with *ProBCCP2* (Figure 4b). Quantitative ß-galactosidase assays performed in yeast cells containing the *lacZ* reporter gene cloned downstream of *ProBCCP2* confirmed these interactions. In these quantitative assays, the reporter activity measured in the presence of MYB118 (Barthole *et al.*, 2014), a member of subgroup S25, was similar to the control, demonstrating a lack of interaction with *ProBCCP2* and establishing the specificity of the interactions observed with the six MYBs composing subgroups S10 and S24 (Figure 4c). Additional experiments carried out with yeast strain AH109 established that all six TFs possessed transcriptional activity (Figure 4d). Finally, transactivation assays in *N. benthamiana* established their ability to activate the *ProBCCP2:uidA* reporter construct, whereas MYB118 (used as a negative control) was not (Figure 4e).

MYB92 activates expression of the *uidA* reporter gene cloned downstream of promoters of various lipogenic genes

As a first approach to evaluate whether MYB92 could activate expression of other lipogenic genes, we considered two Arabidopsis genes for which the expression profiles closely resembled that of *BCCP2* according to Expression Angler 2016 (developmental map; http://bar.utoronto.ca/ExpressionAngler) (Austin *et al.*, 2016) (Figure 5a). These genes coded for the acyl carrier protein 1 (ACP1; At3g05020) and the lipoamide dehydrogenase 1 (LPD1; At3g16950), two components of the FA biosynthetic network. A close examination of proximal upstream regions of these genes allowed identifying AW-boxes and adjacent MYB-core elements that were reminiscent of the structure of *ProBCCP2* (Figure S1). Reporter constructs containing 600 and 515 bp, respectively, of upstream sequences from these genes fused to GUS were used in transactivation assays in *N. benthamiana* leaves. MYB92 was able to specifically activate *ProACP1:uidA* and *ProLPD1:uidA* reporter constructs, showing an important increase in GUS activity compared to the reporters alone or the reporters co-transfected with MYB118 (negative control) (Figure 5b).

Transient expression of *MYB92* in leaves of *N. benthamiana* affects lipid homeostasis and yields a 50-fold increase in suberin deposition

A previous study has described the transcriptional transitions occurring in *N. benthamiana* leaves upon induction of FA synthesis by WRI1 homologs from diverse species (Grimberg *et al.*, 2015). A similar experiment was set up to evaluate the impact of a transient expression of *MYB92*, *WRI1* (positive control) and *MYB118* (negative control) on FA metabolism in *N. benthamiana* leaves. Expression vectors obtained by placing the corresponding cDNAs under the control of the CaMV dual35S promoter were used. Efficient overexpression of the transgenes was checked by a quantitative reverse transcriptase-polymerase chain reaction (qRT-PCR), 5 days after leaf agro-infiltration (Figure 6). Then, the expression levels of several *N. benthamiana* lipogenic genes were quantified. All the glycolytic and FA biosynthetic genes assayed appeared to be upregulated in leaves expressing *WRI1* or *MYB92* with respect to controls. These included the enolase-encoding *ENO1*, the 3-ketoacyl-acyl carrier protein synthase I-encoding *KAS1*, the enoyl-acyl carrier protein reductase-encoding *MOD1*, the lipoamide dehydrogenase-encoding *LPD1*, the acyl carrier protein-encoding *ACP5* and the biotin carboxyl carrier protein subunit-encoding *BCCP2*. For all these genes, increases in transcript levels measured in leaves expressing *WRI1* were two- to five-fold higher than the increases observed in leaves expressing *MYB92*. This induction of lipogenic genes was specific because the relative mRNA

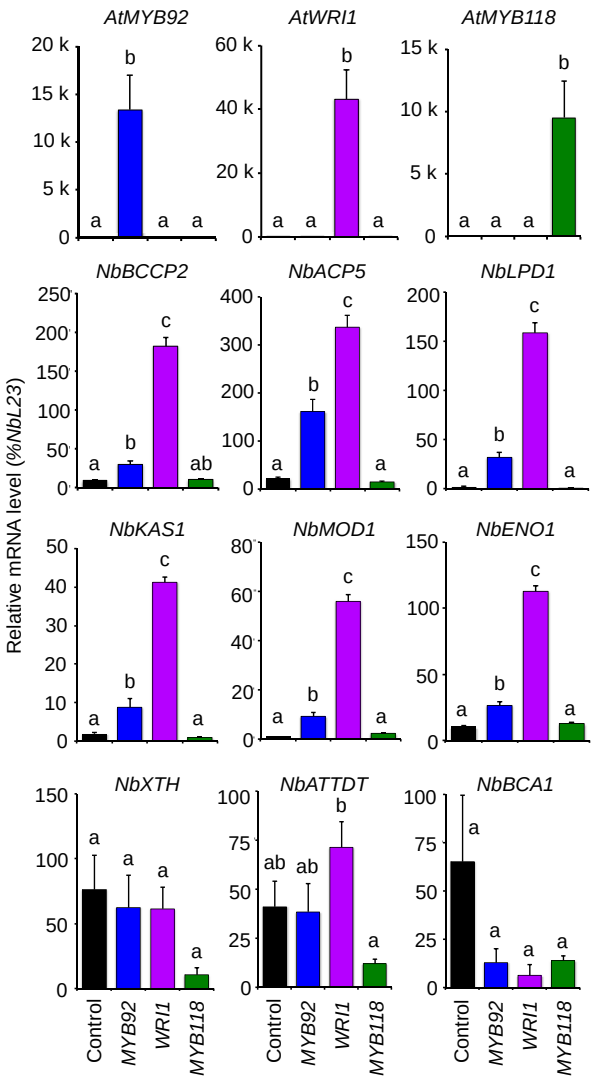

Figure 6. Transcriptional activation of lipogenic genes by MYB92 in leaves of *Nicotiana benthamiana*. A vector allowing the expression of *MYB92*, *WRI1* or *MYB118* was co-infiltrated in young leaves of *N. benthamiana* with a vector coding for the p19 protein. In control leaves, the vector coding for the p19 protein was infiltrated alone. Leaf discs were harvested 4 days after infiltration and cDNAs obtained from six independent mRNA extractions for each vector studied were used for quantitative reverse transcriptase-polymerase chain reaction experiments. Analyses of transcript abundance are presented for Arabidopsis transgenes (*AtMYB92*, *AtWRI1* and *AtMYB118*) and for *N. benthamiana* genes. Values are the means and SE of six or twelve replicates. Statistical analyses of the data were performed using one-way analysis of variance, followed by Tukey's honestly significant difference and Holm–Bonferroni multiple comparison tests ($P < 0.01$).

levels of genes participating in other cellular processes, such as the xyloglucan endotransglucosylase/hydrolase protein 9-encoding *NbXTH*, the dicarboxylate transporter-encoding *NbATTDT* or the beta-carbonic anhydrase-encoding *NbBCA1*, did not display the same pattern (Figure 6).

To evaluate the impact of these transcriptional transitions on lipid homeostasis in transformed leaves, total lipids were extracted from a first set of samples and subjected to thin-layer chromatography to separate polar lipids from triacylglycerols. The two lipid fractions were analyzed separately by gas chromatography (GC) (Figure 7a and Figure S2). In parallel, a second set of leaf samples was subjected to extensive delipidation, and both the amount and composition of residual bound lipids were analyzed by GC-mass spectrometry (MS) (Figure 7b). Expression of *MYB118* in leaves of *N. benthamiana* did not affect lipid homeostasis, Whereas *WRI1* induced triacylglycerol accumulation, as reported previously (Vanhercke *et al.*, 2013; Grimberg *et al.*, 2015). By contrast, expression of *MYB92* yielded a 50-fold increase in the production of surface lipid polyesters. Analysis of the leaf polyester composition revealed aliphatic monomers typical of suberin. Particularly diagnostic of suberin aliphatics were the 223- and 152-fold increases in dicarboxylic C16:0 and C18:1 FA content, respectively, as well as the 130- and 110-fold increases in C22:0 and ω-hydroxy C22:0 FA content, respectively, accompanied by a 17-fold increase in ferulic acid content. The important accumulation of saturated and monounsaturated alcohols and the large proportion of very long-chain monomers ($C \geq 20$) were also strongly indicative of suberin deposition. Importantly, enhancement of polyester production in leaves of *N. benthamiana* by MYB92 had only limited effects, if any, on polar lipid and TAG contents (Figure 7a and Figure S2), suggesting an efficient channeling of the excess FAs produced in the polyester biosynthesis pathway.

Overexpression of *MYB92* in leaves of *N. benthamiana* increases the abundance of suberin biosynthetic gene transcripts

These observations prompted us to analyze the expression of several *N. benthamiana* genes homologous to Arabidopsis genes encoding well-characterized actors of the polyester biosynthetic pathway (Figure 8). In leaves expressing *MYB92*, the 1075- and 75-fold increases in transcript abundance of the ferulate transferase-encoding *ASFT* (Molina *et al.*, 2009) and FA elongase-encoding *KCS1* (Todd *et al.*, 1999) were fully consistent with the accumulation of ferulic acid and monomers with a chain length of >20 carbons, respectively (Figure 7). *CYPB86B1* transcripts were elevated by more than 400-fold, in agreement with the remarkable increase in ω-hydroxy and dicarboxylic FAs. Cytochrome P450 CYP86B1 is responsible for the ω-hydroxylation of very long-chain saturated FAs (Compagnon *et al.*, 2009). Induction of the glycerol-3-phosphate dehydrogenase-encoding *GPDHc1* probably contributed to the production of glycerol backbones. The 120-fold induction of *GPAT5* transcript abundance was probably critical for the proper assembly of suberin considering the importance of glycerol-3-phosphate acyltransferase 5 in the synthesis of *sn*-2 monoacylglycerol intermediates (Beisson

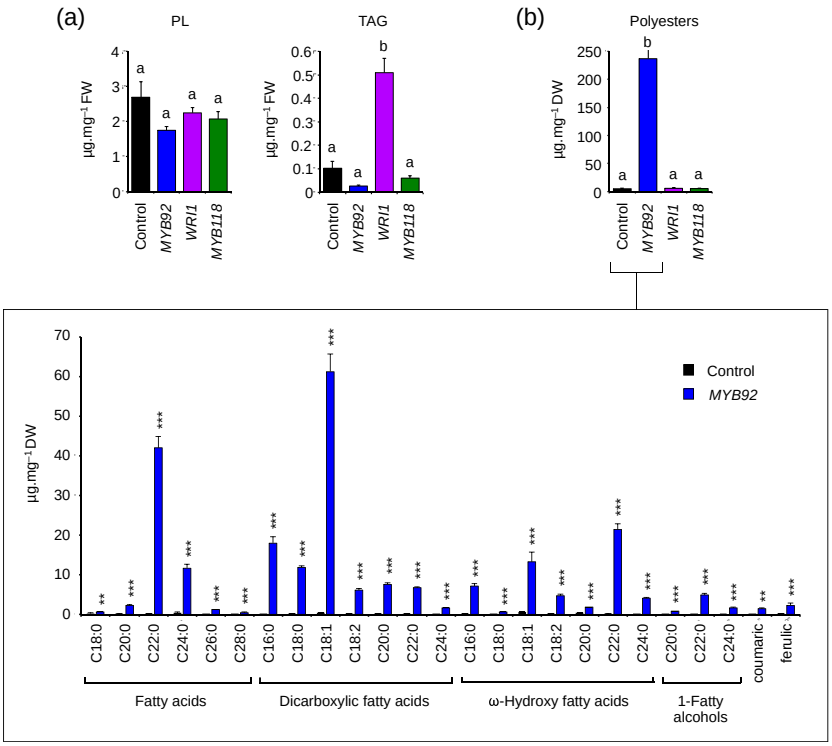

Figure 7. Lipid composition of leaves of *Nicotiana benthamiana* expressing *MYB92*, *WRI1* or *MYB118*. A vector allowing the expression of transcription factors was co-infiltrated in young leaves of *N. benthamiana* with a vector coding for the p19 protein. In control leaves, the vector coding for the p19 protein was infiltrated alone. Leaf discs harvested 4 days after infiltration were used for lipid extractions. (a) Concentrations of polar lipids (PL) and triacylglycerols (TAG) separated by thin-layer chromatography and expressed on a fresh weight (FW) basis. (b) Concentrations of suberin monomers expressed on a dry weight (DW) basis of delipidated material. The detailed composition of leaves expressing *MYB92* is presented: each constituent is designated by carbon chain length and labeled by chemical class along the *x*-axis. Values are the mean ± SE of four (a) or five (b) biological replicates. Statistical analyses of the data (PL, TAG and total polyesters) were performed using one-way analysis of variance, followed by Tukey's honestly significant difference and Holm–Bonferroni multiple comparison tests ($P < 0.01$). In the box presenting concentrations of suberin monomers, asterisks indicate significant difference from the control according to a *t*-test (***$P < 0.001$ and **$P < 0.01$, respectively).

et al., 2007; Yang *et al.*, 2010). In comparison with the strong induction of *GPAT5*, the moderate 18-fold increase in transcript abundance of *GPAT4* measured in leaves expressing *MYB92* might be related to a limited involvement of this acyltransferase in suberin assembly: GPAT4 would also participate in cutin biosynthesis (Kosma *et al.*, 2014). Taken together, these data indicate that overexpression of *MYB92* in leaves of *N. benthamiana* also leads to significant increases in the accumulation of suberin-related biosynthetic gene transcripts. The ability of this TF to activate a wide array of genes involved in late glycolysis, FA and polyester biosynthesis appears as a rare example of transcriptional control able to trigger a whole biosynthetic process, from primary metabolism to the final assembly of a complex polymer made of specialized metabolites.

Effects of stable ectopic expression of *MYB92* in leaves of Arabidopsis

To test the effect of *MYB92* overexpression in the native system, stable *Pro35Sdual:MYB92* lines were generated. Three independent transformants with a single insertion locus were characterized. Homozygous lines were grown under controlled conditions and vegetative growth was not affected in these lines. *MYB92* mRNA level was quantified in rosette leaves of the transgenic lines by qRT-PCR, confirming efficient overexpression of *MYB92* (from 1900 to 2500-fold compared to expression in the wild-type) (Figure 9a). qRT-PCR analyses then established that *BCCP2* and two genes coding for enzymes of the polyester biosynthesis pathway, *ASFT* and *CYP86B1*, were significantly upregulated in the transgenic lines. However, induction levels measured in the native system for *ASFT* and *CYP86B1* were one order of magnitude lower than those observed in *N. benthamiana*. To evaluate the impact of these transcriptional modifications on leaf polyester biosynthesis, delipidated leaf samples were subjected to GC-MS analyses (Figure 9b and Figure S3). Consistent with the upregulation of *CYP86B1A* in transgenic leaves, a limited but significant increase in dicarboxylic FA content could be observed. Beyond these limited compositional changes, polyester biosynthesis was not reoriented toward massive suberin production as in leaves of *N. benthamiana*

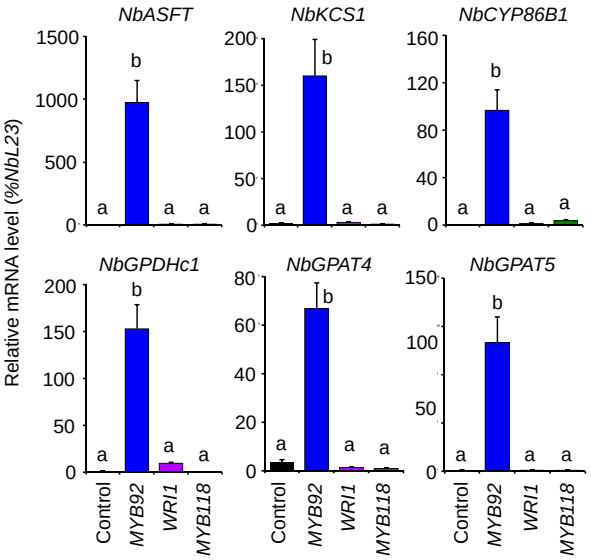

Figure 8. Transcriptional activation of genes involved in suberin biosynthesis by MYB92 in leaves of *Nicotiana benthamiana*. A vector allowing the expression of *MYB92*, *WRI1* or *MYB118* was co-infiltrated in young leaves of *N. benthamiana* with a vector coding for the p19 protein. In control leaves, the vector coding for the p19 protein was infiltrated alone. Leaf discs were harvested 4 days after infiltration and cDNAs obtained from six independent mRNA extractions for each vector studied were used for quantitative reverse transcriptase-polymerase chain reaction experiments. Values are the mean ± SE of six replicates. Statistical analyses of the data were performed using one-way analysis of variance, followed by Tukey's honestly significant difference and Holm–Bonferroni multiple comparison tests ($P < 0.01$).

though. The contrasted responses observed in these two expression systems suggest a need to further examine the post-transcriptional regulation affecting MYB92 activity in Arabidopsis.

DISCUSSION

Regulatory mechanisms modulating the rate of FA biosynthesis and integrating this biochemical process into a developmental framework have long been ignored in plants. Identification of the WRI1 TF was a first, significant step towards the elucidation of the regulation of acyl chain production (Cernac and Benning, 2004). This discovery has emphasized the key role-played by transcriptional regulation in the developmental activation of the FA biosynthetic pathway (Maeo *et al.*, 2009; Baud *et al.*, 2009b). It was then established that the regulatory mechanism involving WRI1 is well conserved among plant species and that plant genomes usually encode several WRI-like TFs with partially redundant functions (Pouvreau *et al.*, 2011; Dussert *et al.*, 2013; Tang *et al.*, 2018). In genetic backgrounds where these WRI regulators are absent, several developmental defects have been reported. In the Arabidopsis *wri1 wri3 wri4* triple mutant, for example, a severe depletion in storage lipid biosynthesis yields wrinkled seeds, whereas defects in cutin deposition in floral tissues increase the susceptibility of flowers to organ fusions, leading to semisterility (To *et al.*, 2012). Yet, mutants deprived of WRI TFs are not lethal and vegetative development of these plants appears to be unmodified under controlled growth conditions, suggesting that FA biosynthesis is not drastically compromised during a large part of the plant life cycle. What is more, the expression of WRI target genes is not completely abolished in *wri* mutant backgrounds. Taken together, these observations suggested that the transcriptional machinery regulating FA biosynthesis might involve additional TFs partially redundant with the WRIs. Accordingly, different types of putative *cis*-acting regulatory elements were shown to be over-represented in FA biosynthesis genes (Peng and Weselake, 2011). Aside from the AW-box motif interacting with the WRIs, binding sites for DOF, GATA and MYB TFs were thus predicted. The functional importance of one of these elements was further confirmed *in planta* by approaches of promoter dissection coupled with site-directed mutagenesis (Baud *et al.*, 2009b).

The yeast one-hybrid screening reported in the present study allowed the identification of MYB92, a TF able to bind the promoter of *BCCP2*. Complementary analyses carried out in yeast and *in planta* then established that the six TFs comprising subgroups S10 (MYB9, MYB107 and MYB30) and S24 (MYB92, MYB53 and MYB93), according to the classification proposed by Dubos *et al.* (2010) for the MYB family, could activate this promoter. These TFs share a highly conserved DNA-binding domain called the MYB domain, consisting of up to four amino acid sequence repeats (R) of approximately 52 residues. MYB TFs from subgroups S10 and S24 belong to the R2R3-MYB class, which gathers most of the plant MYBs (126 out of 196 in Arabidopsis) (Dubos *et al.*, 2010).

Taken together, transactivation of the *BCCP2* promoter in leaves of *N. benthamiana* and *in vitro* binding of MYB92 to the corresponding nucleotidic sequence strongly suggest that MYB92 directly binds to this promoter *in planta*. If many R2R3-MYBs usually recognize DNA motifs enriched in adenosine and cytosine residues (called AC elements), the range of their binding sites remains poorly described *in planta* (Prouse and Campbell, 2012). Our data suggest that the GTTTGGT and GTTAGTT elements can be part of the *in vivo* MYB92 binding site(s). The reverse complement of the first element identified (ACCAAAC) is also found in the *cis*-element bound by MYB61 as defined by cyclic amplification and selection of targets (Prouse and Campbell, 2013). The sequence is also very similar to the secondary wall MYB-responsive element (SMRE) bound by MYB46 and MYB83 (ACC[A/T]A[A/C][T/C]) and identified by promoter deletion and EMSA (Zhong and Ye, 2012). The second element is found in the consensus sequence of MBSII (aaaAGTTAGTTA), a MYB DNA-binding site of

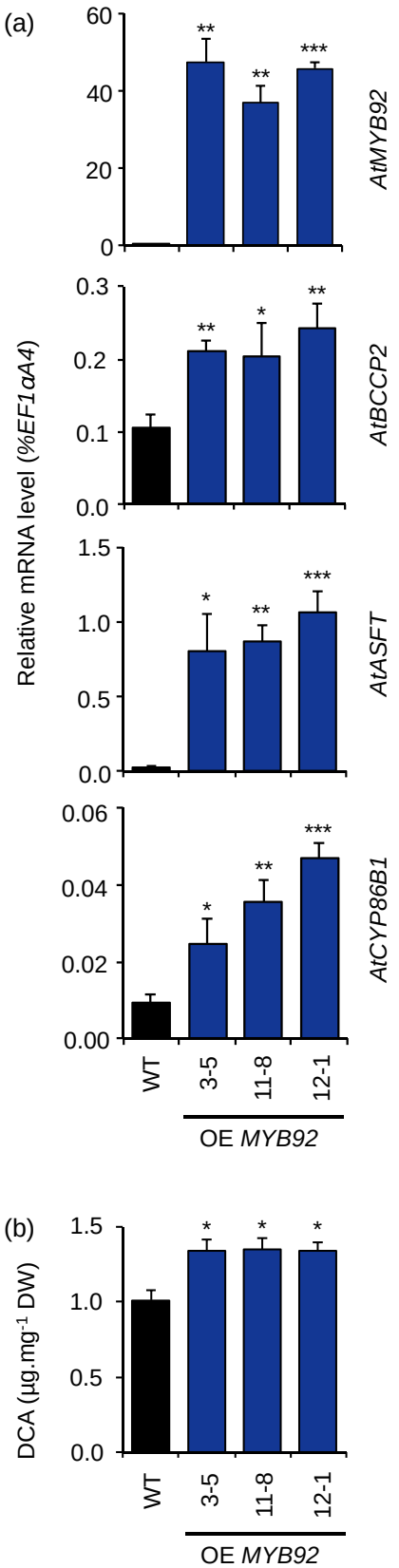

Figure 9. Characterization of leaves of *Arabidopsis thaliana* stably overexpressing *MYB92*. (a) Quantitative reverse transcriptase-polymerase chain reaction analysis of transcript abundance in cDNAs prepared from rosette leaves. Values are the mean ± SE of three to six replicates performed on cDNA dilutions obtained from three independent RNA extractions. (b) Content of dicarboxylic fatty acid (DCA) monomers in leaf polyesters as determined by gas chromatography-mass spectrometry and expressed on a dry weight of delipidated material. Values are the mean ± SE of three to five replicates. Asterisks indicate a significant difference from the wild-type (WT) control according to a *t*-test (***$P < 0.001$, **$P < 0.01$ and *$P < 0.05$, respectively).

MYB.Ph3 from *Petunia hybrida* identified by EMSA (Solano *et al.*, 1995). This sequence also fits the position weight matrices representing top-scoring 8-mers for MYB46, MYB52, MYB55, MYB59 and MYB11 as defined by protein-binding microarray approaches (Franco-Zorrilla *et al.*, 2014). If the two elements bound by MYB92 are not identical, site-directed mutagenesis experiments have highlighted common nucleotides within these two elements that are critical for MYB92 binding (Figure 2c). Extensive characterization of DNA-binding specificities of plant TFs has revealed that an unexpectedly elevated number of TFs, including members of the MYB family, can recognize secondary *cis*-acting regulatory elements with similar or slightly lower affinities to their primary ones (Franco-Zorrilla *et al.*, 2014). Secondary motifs usually represent sequence variants of the primary elements. A more detailed structure-function study using *in vitro* and *in vivo* techniques such as SPR (surface plasmon resonance), SELEX (systematic evolution of ligands by exponential enrichment), protein-binding microarray or chromatin immunoprecipitation will be necessary to comprehensively characterize the MYB92 DNA-binding matrix(ces).

The data obtained both *in vitro* and *in planta* emphasize the importance of the concomitant presence of two adjacent MYB *cis*-elements for the binding and transcriptional activation of the promoter of *BCCP2* by MYB92. It is possible that MYB92 proteins interact with the promoter as dimers. If further studies are now required to test this hypothesis, examples of MYB dimerization have already been reported for MYB123 (TT2), involved in the production of condensed tannins (Baudry *et al.*, 2004), MYB21 and MYB24, which regulate jasmonate-mediated stamen development (Huang *et al.*, 2017), or BpMYB46, involved in the response to abiotic stresses in *Betula platyphylla* (Wang *et al.*, 2019). According to the supershifted bands observed in EMSA experiments (Figure 1d), the 15 nucleotides separating the MYB *cis*-elements bound by MYB92 from the AW motif recognized by WRI1 allow the simultaneous presence of the two types of TFs on the promoter of *BCCP2*. The results obtained within the frame of the present study show that they can bind and activate the promoter of *BCCP2* independently from each other and that

they do not activate the promoters of FA biosynthetic genes with the same efficiency. Both in yeast one-hybrid assays and in transient activation assays carried out in leaves of *N. benthamiana*, expression of *WRI1* yielded a stronger activation of these target promoters. Considering that *wri1 myb92* mutant seeds exhibit the same phenotype as *wri1* seeds (Figure S4), it is unlikely that MYB92 and WRI1 have redundant functions in the oil-accumulating tissues of the seed.

The qRT-PCR approaches carried out in leaves of *N. benthamiana* and Arabidopsis overexpressing *MYB92* have unraveled a second subset of target genes specifically activated by the TF. This subset comprises genes characteristic of the suberin aliphatic polyester biosynthesis pathway such as *ASFT*, *CYP86B1* or *GPAT5*. Interestingly, increases in the corresponding transcript levels upon *MYB92* expression were at least one order of magnitude higher than the increases in the accumulation of FA biosynthetic transcripts measured in the same samples. It is tempting to speculate that MYB92 regulates these different gene subcircuits by means of distinct regulatory mechanisms. Secondary cell wall synthesis (Zhong *et al.*, 2010) and triacylglycerol production in maturing seeds (Baud and Lepiniec, 2009) were also shown to require the concerted activation of different gene subcircuits through different molecular mechanisms. Some of these mechanisms involve indirect regulation by means of secondary TFs participating in downstream cascades of transcriptional activation. Regarding the regulation of suberin biosynthesis, the existence of such cascades cannot be completely ruled out. However, the present study provides evidence that MYB TFs comprising subgroups S10 and S24 directly activate the FA biosynthesis gene *BCCP2*, whereas Gou *et al.* (2017) reported a direct transcriptional activation of suberin biosynthesis genes by MYB107. Taken together, these results invite us to consider other types of mechanisms regulating the concerted activation of these pathways. For example, differential protein–protein interactions could specify the binding of the TFs to their target promoters or modulate their transcriptional activity. Importantly, the regulatory cascades hypothesis and the occurrence of differential protein-protein interactions are not necessarily mutually exclusive, considering that some TFs can directly control the expression of genes coding for their own protein partners. This can be exemplified by the regulation of the synergid gene regulatory network by MYB98 (Punwani *et al.*, 2008). Identification of interacting partners of the MYB TFs considered in the present study, combined with an in-depth characterization of the promoter sequences of the suberin biosynthesis genes, will be essential for further elucidating the complex regulatory network governing the synthesis of these polyesters.

Suberin is an acylglycerol polymer deposited on the inner surface of the cell wall of specific cell types forming a secondary wall structure, in certain endodermal and peridermal tissues (Kosma *et al.*, 2014; Jenkin and Molina, 2015). Suberized tissues include seed coat layers, tree bark, periderms of tubers and roots, root endodermis, and abscission scars (Franke and Schreiber, 2007; Franke *et al.*, 2012). This polyester is also deposited in response to wounding (Boher *et al.*, 2013). Ectopic expression of *MYB92* in leaves of *N. benthamiana* is sufficient to trigger the massive production and deposition of suberin-type monomers such as 18:1 and very long-chain saturated ω-hydroxy and dicarboxylic FAs. Further studies are now required for a comprehensive understanding of the physiological functions and the regulation of this TF in Arabidopsis. Expression of *MYB92* in the endodermis of the root of Arabidopsis (Iyer-Pascuzzi *et al.*, 2011) suggests a role in the regulation of the biosynthesis of Casparian strips. Although seed expression of *MYB92* (Figure S4) may coincide with suberin deposition, a thorough characterization of *myb92* mutant seeds did not allow detecting any defect in polyester accumulation in this organ (Figure S4). It is likely that MYB92 and closely related MYB transcription factors have partially redundant functions with respect to polyester synthesis, and that functionally redundant and coexpressed MYBs hamper approaches of reverse genetics.

In agreement with this hypothesis, MYB9 and MYB107 were previously shown to regulate suberin deposition in the integument of Arabidopsis seeds. Similarly, MYB TFs homologous to Arabidopsis MYB factors from subgroups S10 and S24 were also linked to suberin biosynthesis across multiple plant species (Legay *et al.*, 2016; Lashbrooke *et al.*, 2016; Gou *et al.*, 2017). However, transcriptional regulation of suberin deposition by MYB TFs appears to involve an even wider array of MYB factors because MYB41, a member of adjacent subgroup S11, can activate suberin synthesis under conditions of abiotic stress (Kosma *et al.*, 2014). The reason why several related TFs participate in the regulation of the same pathway in a given plant species could be a result of the need to integrate a variety of developmental and environmental signals; hence, the partially different expression patterns of the genes encoding these factors (Winter *et al.*, 2007; Gibbs *et al.*, 2014; Kosma *et al.*, 2014; Gou *et al.*, 2017).

It is tempting to propose that these factors do not activate the same array of targets in exactly the same manner, allowing a modulation of the polyester composition as a result of subtle variations in the activation of enzymes participating in the biosynthesis pathway. In agreement with this, analysis of the suberin monomers in different organs of Arabidopsis (e.g. seed integuments and roots) reveals strikingly different compositions (Li-Beisson *et al.*, 2010). This hypothesis is also supported by the occurrence of cutin regulators (MYB16 and MYB106) in the adjacent subgroup 9 of MYB TFs that induce the production of a

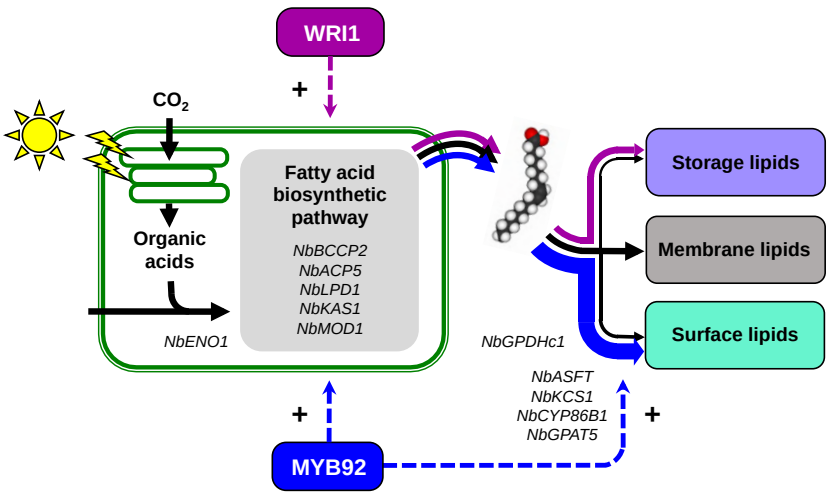

Figure 10. Model for the transcriptional regulation of lipid homeostasis in leaves of *Nicotiana benthamiana*. In wild-type leaves, fatty acids produced in the plastids are mainly used for membrane lipid synthesis and, to a lesser extent, for the production of surface and storage lipids. Upon *WRI1* expression, the fatty acid biosynthetic pathway is upregulated. However, WRI1 does not dictate the use made of these excess fatty acids. It appears that triacylglycerol biosynthetic enzymes coded by genes already expressed in untransformed leaves efficiently channel excess fatty acids toward triacylglycerol production, leading to a limited but significant over accumulation of storage lipids. By contrast, MYB92 not only activates glycolytic and fatty acid biosynthetic genes, but also targets genes coding for suberin biosynthetic enzymes. As a consequence, a remarkable increase in suberin monomers is measured in leaves expressing *MYB92*.

glycerolipid polyester related to suberin, despite characteristic differences in chemical composition (Oshima *et al.*, 2013; Jenkin and Molina, 2015).

The discovery that *MYB93* expression in endodermal cells also participates in the regulation of lateral root development through interaction with ARABIDILLO proteins (Gibbs *et al.*, 2014) suggests another explanation for the multiplication of MYB factors regulating polyester biosynthesis. It could well be that some of these MYBs act as master regulators governing the metabolic and developmental processes required for the specialization of different cell types producing suberin. Different MYB factors interacting with distinct protein partners may lead to the specification of different cell fates.

In conclusion, we have demonstrated that MYB92 is capable of activating FA biosynthetic genes. Expression of *WRI1* in leaves of *N. benthamiana* stimulates FA synthesis and promotes TAG accumulation, whereas expression of *MYB92* in the same system yields a remarkable accumulation of suberin (Figure 10). This efficient channeling of FAs in the polyester biosynthetic pathway relies on the strong transcriptional activation of the actors of the pathway also regulated by MYB92. The demonstration that MYB92, similar to MYB41 (Kosma *et al.*, 2014), can stimulate the ectopic deposition of suberin-type material provides an original tool for the biotechnological design of crops with improved agronomical properties linked to altered barrier properties. This could also serve as a lever for the production of renewable chemical feedstock, thus contributing to replace fossil oil for some material and chemicals for the industry (Gandini, 2008). Both basic and applied research objectives now require an exhaustive characterization of these closely related MYB TFs to elucidate their specificities and regulation.

EXPERIMENTAL PROCEDURES

Constructs

The sequences of primers used for DNA amplification are provided in Table S1.

For construction of the *Pro35Sdual:MYB* transgenes, *MYB92* and *MYB107* cDNAs were amplified with the proofreading Phusion High-Fidelity DNA polymerase (Thermo Scientific, Waltham, MA, USA) from a mixture of seed cDNAs (Col-0 accession). The PCR products were introduced by BP recombination into the pDONR207 entry vector (Invitrogen, Carlsbad, CA, USA). Kelemen *et al.* (2015) previously reported the cloning of *MYB9*, *MYB39*, *MYB53* and *MYB93* cDNAs into pDONR207. The cDNAs were then transferred into the destination vector pMDC32 (Curtis and Grossniklaus, 2003) by LR recombination.

Construction of the *Pro35Sdual:WRI1* transgene was described previously by Baud *et al.* (2007a) in addition to that of the *Pro35Sdual:MYB118* transgene by Barthole *et al.* (2014).

For construction of the *ProACP1:uidA* and *ProLPD1:uidA* transgenes, regions −600 to −1 bp and −515 to −1 bp relative to the translational start codon of the genes considered were amplified with the proofreading Phusion High-Fidelity DNA polymerase (Thermo Scientific) from Col-0 genomic DNA. The PCR products were introduced by BP recombination into the pDONR207 entry vector (Invitrogen) and transferred into the destination vector pBI101-R1R2-GUS (Baud *et al.*, 2007a) by LR recombination.

Construction of the *ProBCCP2:uidA* transgene was described previously by Baud *et al.* (2009b) in addition to that of the *ProODD:uidA* transgene by Barthole *et al.* (2014).

For construction of the *Pro35Sdual:MYB92:mGFP6* transgene, *MYB92* cDNA without STOP codon was amplified with the proofreading Phusion High-Fidelity DNA polymerase (Thermo Scientific) from a mixture of seed cDNAs (Col-0 accession). The PCR

product was introduced by BP recombination into the pDONR207 entry vector and transferred into the destination vector pMDC83 (Curtis and Grossniklaus, 2003) by LR recombination.

For construction of the *ProADH1:GAL4-DBD:MYB* transgenes, cDNAs previously cloned into the pDONR207 entry vector were transferred into the pDEST32 vector for GAL4-DBD fusion (Invitrogen).

RNA analysis

The material used for RNA extraction was frozen in liquid nitrogen immediately after harvest, then stored at −80°C. RNA extraction and reverse transcription were carried out as described previously (Baud *et al.*, 2004).

RT-PCR analyses were performed as described in Baud *et al.* (2004). Primers used for RT-PCR (Figure S2) were: 5′-ATGGGAAGATCTCCTATCTC-3′ (*MYB92*_atg) and 5′-CTAAGGAATGTCGGAAAATA-3′ (*MYB92*_stop), 5′-ATGCCCCAGGACATCGTGATTTCAT-3′ (*EF*_up) and 5′-TTGGCGGCACCCTTAGCTGGATCA-3′ (*EF*_low).

Real-time qRT-PCR reactions were performed in a CFX Connect Real-Time PCR Detection System (Bio-Rad, Hercules, CA, USA), using the SsoAdvanced PreAmp Supermix Bio-Rad kit in accordance with the manufacturer's instructions. Reactions used 5 μl of 1:50 diluted cDNAs in a total volume of 15 μl. Incubation of the reactions comprised: a first step at 95°C for 8 min to activate the hot start recombinant Taq DNA polymerase, followed by 40 cycles of 95°C for 10 sec and 60°C for 10 sec. The specificity of the PCR amplification was checked with a heat dissociation protocol (from 60 to 95°C with a temperature transition rate of 0.1°C sec^{-1}) following the final cycle of the PCR. The efficiency of the primer sets was calculated by performing a RT-PCR on several dilutions of first strands. Efficiencies of the different primer sets used were confirmed to be almost similar. The results obtained for the different *N. benthamiana* samples analyzed were standardized to the constitutive *NbL23* gene (coding for a 60S ribosomal protein) expression level (Liu *et al.*, 2102). Those obtained for the *A. thaliana* samples analyzed were standardized to the constitutive *EF1αA4* gene (coding for a translation elongation factor) expression level (Nesi *et al.*, 2000). The sequences of primers used for real-time qRT-PCR are provided in Table S2.

Yeast one-hybrid experiments

Construction of the pHISi reporter plasmid containing a 180-bp fragment of the *BCCP2* promoter was described previously by Baud *et al.* (2009b). Integration of the plasmid into the yeast strain EGY48 and screening of the REGIA cDNA expression library were described previously by To *et al.* (2012).

To validate the candidate genes isolated, *MYB* cDNAs were cloned into the pDEST22 vector (Invitrogen) to be expressed in yeast as GAL4 AD fusions. cDNAs previously cloned into the pDONR207 were transferred into the pDEST22 expression vector by LR recombination. YM4271 yeast cells presenting the *HIS3* reporter gene under the control of a functional *BCCP2* promoter (To *et al.*, 2012) were transformed with pDEST22 in accordance with the AcLi/SSDNA/PEG method (Gietz and Woods, 2002). Transformants were selected on appropriate media. Construction of *ProBAN:HIS* was described previously (Baudry *et al.*, 2004).

The reporter plasmid used for ß-galactosidase assays was constructed by insertion of a 180-bp fragment of the *BCCP2* promoter into the pLacZi vector (To *et al.*, 2012). After digestion with *Apa*I, this plasmid was integrated into the yeast strain YM4271 at the *URA3* locus. The resulting yeast strains were selected on a medium lacking uracil and then co-transformed with the pDEST22 vector allowing expression of the MYBs using the AcLi/SSDNA/PEG method (Gietz and Woods, 2002). Transformants were selected on appropriate media and ß-galactosidase activity was assayed on liquid cultures using o-nitrophenyl-ß-D-galactopyranoside as a substrate, as recommended by the constructor (Yeast protocol handbook; Clontech, Palo Alto, CA, USA).

Electrophoretic mobility shift assays

The expression plasmid was constructed by transferring *MYB92* cDNA from the pDONR207 to the expression vector pETG20A (http://www/embl-hamburg.de). The resulting vector was electroporated into *Escherichia coli* RosettaBlue(DE3)pLysS strain (Novagen, Madison, WI, USA) for expression. After induction by 0.5 mM isopropyl β-D-1-thiogalactopyranoside in Luria Bertani buffer, cells were grown overnight at 17°C. Cell lysis and protein purification were adapted from Baud *et al.* (2009b). Briefly, cell pellet was sonicated in lysis buffer A (20 mM NaCl, 20 mM Tris-HCl, pH 8.0, 5 mM imidazole, 5% glycerol) and centrifuged for 40 min at 21 000 ***g***. The clear supernatant was incubated for 4 h at 4°C with Ni-NTA resin (Qiagen, Valencia, CA, USA). The resin was transferred into a column, washed with 5 ml of buffer A plus 20 mM imidazole and eluted with 5 ml of buffer A plus 300 mM imidazole. Recombinant WRI1 and LEC2 proteins were obtained as described previously in Baud *et al.* (2009b) and Baud *et al.* (2009a), respectively.

To prepare DNA probes, complementary biotin-labeled (at the 5′ end) oligonucleotides (Eurofins MWG Operon, Louisville, KY, USA) were annealed. The DNA-binding assays were performed as described previously in Troncoso-Ponce *et al.* (2016).

Lipid analysis

To analyze polar lipids and triacylglycerols, 500 mg of leaves was harvested and stored at −80°C prior to lipid extraction. Leaf samples were ground in 7.2 ml of pre-cooled chloroform/methanol/formic acid (10:10:0.5, v/v/v) and incubated at −20°C overnight. The mixture was centrifuged at 7500 ***g*** for 10 min at 4°C to pellet the cell debris. Lipids of the pellet were reextracted in 2.64 ml of pre-cooled chloroform/methanol/water (10:10:1, v/v/v). Then, 3.6 ml of cooled Hajra solution (KCl 2 M and H_3PO_4 0.2 M) were added to the pooled supernatants. After shaking and centrifugation (7500 ***g*** for 10 min at 4°C), the lower phase containing lipids was collected and evaporated with a stream of N_2. Lipids were finally resuspended in chloroform/methanol (2:1, v/v) and separated on thin-layer chromatography plates developed with hexane/diethylether/acetic acid (35:15:0.01, v/v/v). Polar lipids and triacylglycerols were visualized under UV by staining with sprayed primuline. Lipid spots were ultimately collected and analyzed by GC as described previously (Baud *et al.*, 2002).

To analyze suberin polyester composition in leaves, fresh material was collected and immersed in hot isopropanol for 10 min at 80°C. For seed coat analyses, 50 mg of dry seeds was ground in isopropanol, and then heated for 3 h at 85°C. After cooling, samples were extensively delipidated by extracting the soluble lipids, then dried and depolymerized as described previously (Domergue *et al.*, 2010). Extraction, derivatization, and analysis by GC-MS were performed as described previously (Domergue *et al.*, 2010).

For determination of seed oil content, total fatty acid analyses were performed on pools of 20 dry seeds as described previously (Li *et al.*, 2006).

Microscopy

Histochemical detection of GUS activity and bright-field microscopy observations of leaf discs were performed as described by

Baud *et al.* (2007b). MYB92-GFP fusion proteins were imaged in leaves of *N. benthamiana* with a LSM710 confocal microscope (Carl Zeiss, Oberkochen, Germany) as described by Miart *et al.* (2014).

Molecular characterization of T-DNA mutants

Plant genomic DNA flanking the left T-DNA borders of the T-DNA mutant lines ordered from the Salk Institute (La Jolla, CA, USA) were amplified by PCR and sequenced to confirm the flanking sequence tags identified. Molecular characterization of the *wri1-4* allele was described previously (Baud *et al.*, 2007a). In the *myb92-1* line (N116918), the T-DNA insertion was located in the third exon of the *MYB92* gene. To amplify the T-DNA left border, pAt5g10280F (5′-GCAAGCAACCAAATCTCAGAG-3′) and JicSMLB2 (5′- CGAATAAGAGCGTCCATTTTAGAG-3′) were used. To amplify the left T-DNA border in *myb92-2* (N128394; insertion located in the second exon of the *MYB92* gene), pAt5g10280F and JicSMLB2 were used. In the *myb107* line (N107792), the T-DNA insertion was located in the second exon of the *MYB107* gene. To amplify the T-DNA left border, At3g02940R (5′-ATGGCTGGTGATCTTGTGTA-3′) and JicSMLB2 were used.

Seed coat permeability test

Tetrazolium red assays used for seed coat permeability tests were performed as described previously (Vishwanath *et al.*, 2013). Dry seeds were incubated in the dark in a solution of 1% (w/v) tetrazolium red (2,3,5-triphenyltetrazolium chloride) at 30°C for 48 h. The seeds were observed for a change in color using a binocular magnifier.

Phylogenetic analysis

To perform distance analysis among the MYB TFs, programs (with default values) available via https://mafft.cbrc.jp/alignment/server were used: MAFFT, version 7 for multiple alignments and NJ (neighbor-joining, with 1000 bootstraps) for tree building (Kuraku *et al.*, 2013). Alignments are provided in Figure S5.

Materials described in this manuscript will be available on request.

ACCESSION NUMBERS

Arabidopsis sequence data from the present study are available in the EMBL/GenBank data libraries under accession numbers: *AtACP1*, At3g05020; *AtASFT*, At5g41040; *AtBAN*, At1g61720; *AtBCCP2*, At5g15530; *AtCYP86B1*, At5g23190; *AtEF1αA4*, At5g60390; *AtLPD1*, At3g16950; *AtMYB9*, At5g16770; *AtMYB39*, At4g17785; *AtMYB53*, At5g65230; *AtMYB92*, At5g10280; *AtMYB93*, At1g34670; *AtMYB107*, At3g02940; *AtMYB118*, At3g27785; *AtODD*, At1g04380; *AtWRI1*, At3g54320; *AtWRI3*, At1g16060. *Nicotiana benthamiana* sequence data are available in the Sol Genomics Network data libraries under the accession numbers provided in Table S2.

ACKNOWLEDGEMENTS

We are grateful to Martine Miquel, Zsolt Kelemen, Frédéric Domergue and Christian Dubos for helpful discussions. Vincent Colot is acknowledged for providing the REGIA library. This work was supported by the Agence Nationale de la Recherche (ANR-10-GENM-009 to S.B.; the IJPB benefits from the support of Saclay Plant Sciences-SPS ANR-17-EUR-0007). This work has benefited from the support of IJPB's Plant Observatory technological platforms. Suberin analyses were carried out at Metabolome facility of Bordeaux (https://cgfb.u-bordeaux.fr).

CONFLICT OF INTEREST

The authors declare no conflict of interest.

AUTHOR CONTRIBUTIONS

AT, JJ, LL and SB Conceived and designed the experiments. AT, JJ, JT and SK performed the experiments. AT, JJ, LL and SB analyzed the data. SB conceived and wrote the paper.

SUPPORTING INFORMATION

Additional Supporting Information may be found in the online version of this article.

Figure S1. Schematic representation of the promoter fragments of *BCCP2*, *ACP1*, and *LPD1* used to prepare constructs consisting of the *uidA* reporter gene driven by these different promoters.

Figure S2. Fatty acid composition of leaves of *Nicotiana benthamiana* expressing *MYB92*, *WRI1* or *MYB118*.

Figure S3. Complementary information for the characterization of polyester monomer concentrations in leaves of *Arabidopsis thaliana* stably overexpressing *MYB92*.

Figure S4. Characterization of *myb92* mutant alleles.

Figure S5. Alignment of amino acid sequences corresponding to the MYB transcription factors of subgroups S10 and S24.

Table S1. Primers used for construct preparation.

Table S2. Primers used for quantitative RT-PCR.

REFERENCES

Andre, C., Haslam, R.P. and Shanklin, J. (2012) Feedback regulation of plastidic acetyl-CoA carboxylase by 18:1-acyl carrier protein in *Brassica napus*. *Proc. Natl Acad. Sci. USA*, **25**, 10107–10112.

Austin, R., Hiu, S., Waese, J. *et al.* (2016) New BAR tools for mining expression data and exploring *Cis*-elements in *Arabidopsis thaliana*. *Plant J.* **88**, 490–504.

Barthole, G., To, A., Marchive, C., Brunaud, V., Soubigou-Taconnat, L., Berger, N., Dubreucq, B., Lepiniec, L. and Baud, S. (2014) MYB118 represses endosperm maturation in seeds of *Arabidopsis*. *Plant Cell*, **26**, 3519–3537.

Baud, S. (2018) Seeds as oil factories. *Plant Reprod.* **3**, 213–235.

Baud, S. and Lepiniec, L. (2009) Regulation of *de novo* fatty acid synthesis in maturing oilseeds of *Arabidopsis*. *Plant Physiol. Biochem.* **47**, 448–455.

Baud, S., Boutin, J.-P., Miquel, M., Lepiniec, L. and Rochat, C. (2002) An integrated overview of seed development in *Arabidopsis thaliana* ecotype WS. *Plant Physiol. Biochem.* **40**, 151–160.

Baud, S., Vaultier, M.-N. and Rochat, C. (2004) Structure and expression profile of the sucrose synthase multigene family in Arabidopsis. *J. Exp. Bot.* **55**, 397–409.

Baud, S., Santos Mendoza, M., To, A., Harscoët, E., Lepiniec, L. and Dubreucq, B. (2007a) WRINKLED1 specifies the regulatory action of LEAFY COTYLEDON2 towards fatty acid metabolism during seed maturation in Arabidopsis. *Plant J.* **50**, 825–838.

Baud, S., Wuillème, S., Dubreucq, B., de Almeida, A., Vuagnat, C., Lepiniec, L., Miquel, M. and Rochat, C. (2007b) Function of plastidial pyruvate kinase in seeds of *Arabidopsis thaliana*. *Plant J.* **52**, 405–419.

Baud, S., Reinhard Dichow, N., Kelemen, Z. *et al.* (2009a) Regulation of HSD1 in seeds of *Arabidopsis thaliana*. *Plant Cell Physiol.* **50**, 1463–1478.

Baud, S., Wuillème, S., To, A., Rochat, C. and Lepiniec, L. (2009b) Role of WRINKLED1 in the transcriptional regulation of glycolytic and fatty acid biosynthetic genes in Arabidopsis. *Plant J.* **60**, 933–947.

Baudry, A., Heim, M.A., Dubreucq, B., Caboche, M., Weisshaar, B. and Lepiniec, L. (2004) TT2, TT8, and TTG1 synergistically specify the expression of *BANYULS* and proanthocyanidin biosynthesis in *Arabidopsis thaliana*. *Plant J.* **39**, 366–380.

Beisson, F., Li, Y., Bonaventure, G., Pollard, M. and Ohlrogge, J. (2007) The acyltransferase GPAT5 is required for the synthesis of suberin in seed coats and root of Arabidopsis. *Plant Cell*, **19**, 351–368.

Boher, P., Serra, O., Soler, M., Molinas, M. and Figueras, M. (2013) The potato suberin feruloyl transferase FHT which accumulates in the phellogen is induced by wounding and regulated by abscisic and salicylic acids. *J. Exp Bot.* **64**, 3225–3236.

Bourgis, F., Kilaru, A., Cao, X., Ngando-Ebongue, G.F., Drira, N., Ohlrogge, J.B. and Arondel, V. (2011) Comparative transcriptome and metabolite analysis of oil palm and date palm mesocarp that differ dramatically in carbon partitioning. *Proc. Natl Acad. Sci. USA*, **108**, 12527–12532.

Cernac, A. and Benning, C. (2004) WRINKLED1 encodes an AP2/EREB domain protein involved in the control of storage compound biosynthesis in Arabidopsis. *Plant J.* **40**, 575–585.

Compagnon, V., Diehl, P., Benveniste, I., Meyer, D., Schaller, H., Schreiber, L., Franke, R. and Pinot, F. (2009) CYP86B1 is required for very long chain ω-hydroxyacid and α, ω-dicarboxylic acid synthesis in root and seed suberin polyester. *Plant Physiol.* **150**, 1831–1843.

Curtis, M.D. and Grossniklaus, U. (2003) A gateway cloning vector set for high-throughput functional analysis of genes *in planta*. *Plant Physiol.* **133**, 462–469.

Delude, C., Moussu, S., Joubès, J., Ingram, G. and Domergue, F. (2016) Plant surface lipids and epidermis development. *Subcell. Biochem.* **86**, 287–313.

Domergue, F., Vishwanath, S.J., Joubès, J. *et al.* (2010) Three Arabidopsis fatty acyl-coenzyme A reductases, FAR1, FAR4, and FAR5, generate primary fatty alcohols associated with suberin deposition. *Plant Physiol.* **153**, 1539–1554.

Dubos, C., Stracke, R., Grotewold, E., Weisshaar, B., Martin, C. and Lepiniec, L. (2010) MYB transcription factors in *Arabidopsis*. *Trends Plant Sci.* **15**, 573–581.

Dussert, S., Guerin, C., Andersson, M., Joët, T., Tranbarger, T.J., Pizot, M., Sarah, G., Omore, A., Durand-Gasselin, T. and Morcillo, F. (2013) Comparative transcriptome analysis of three oil palm fruit and seed tissues that differ in oil content and fatty acid composition. *Plant Physiol.* **162**, 1337–1358.

Feria Bourrellier, A.B., Valot, B., Guillot, A., Ambard-Bretteville, F., Vidal, J. and Hodges, M. (2010) Chloroplast acetyl-CoA carboxylase activity is 2-oxoglutarate regulated by interaction of PII with the biotin carboxyl carrier subunit. *Proc. Natl Acad. Sci. USA*, **107**, 502–507.

Franco-Zorrilla, J.M., Lopez-Vidriero, I., Carrasco, J.L., Godoy, M., Vera, P. and Solano, R. (2014) DNA-binding specificities of plant transcription factors and their potential to define target genes. *Proc. Natl Acad. Sci. USA*, **111**, 2367–2372.

Franke, R.B. and Schreiber, L. (2007) Suberin – a biopolyester forming apoplastic plant interfaces. *Curr. Opin. Plant Biol.* **10**, 252–259.

Franke, R.B., Dombrink, I. and Schreiber, L. (2012) Suberin goes genomics: use of short living plants to investigate a long lasting polymer. *Front. Plant Sci.* **3**, 4.

Gandini, A. (2008) Polymers from renewable resources: a challenge for the future of macromolecular materials. *Macromolecules*, **41**, 9491–9504.

Gibbs, D.J., Voß, U., Harding, S.A. *et al.* (2014) ArMYB93 is a novel negative regulator of lateral root development in Arabidopsis. *New Phytol.* **203**, 1194–1207.

Gietz, R.D. and Woods, R.A. (2002) Transformation of yeast by lithium acetate/single-stranded carrier DNA/polyethylene glycol methods. *Methods Enzymol.* **350**, 87–96.

Girke, T., Todd, J., Ruuska, S., White, J., Benning, C. and Ohlrogge, J. (2000) Microarray analysis of developing seeds. *Plant Physiol.* **124**, 1570–1581.

Gou, M., Hou, G., Yang, H., Zhang, X., Cai, Y., Kai, G. and Liu, C.-J. (2017) The MYB107 transcription factor positively regulates suberin biosynthesis. *Plant Physiol.* **173**, 1045–058.

Grimberg, A., Carlsson, S.S., Marttila, S., Bhalerao, R. and Hofvander, P. (2015) Transcriptional transitions in *Nicotiana benthamiana* leaves upon induction of oil synthesis by WRINKLED1 homologs from diverse species and tissues. *BMC Plant Biol.* **15**, 192.

Guerin, C., Joët, T., Serret, J. *et al.* (2016) Gene coexpression network analysis of oil biosynthesis in an interspecific backcross of oil palm. *Plant J.* **87**, 423–441.

Harwood, J. (1996) Recent advances in the biosynthesis of plant fatty acids. *Biochim. Biophys. Acta*, **1301**, 7–56.

Huang, H., Gao, H., Liu, B., Qi, T., Tong, J., Xiao, L., Xie, D. and Song, S. (2017) *Arabidopsis* MYB24 regulates jasmonate-mediated stamen development. *Front. Plant Sci.* **8**, 1525.

Iyer-Pascuzzi, A.S., Jackson, T., Cui, H., Petricka, J.J., Busch, W., Tsukagoshi, H. and Benfey, P.N. (2011) Cell identity regulators link development and stress responses in the Arabidopsis root. *Dev. Cell*, **21**, 770–782.

Jenkin, S. and Molina, I. (2015) Isolation and compositional analysis of plant cuticle lipid polyester monomers. *J. Vis. Exp.* **105**, e53386.

Kelemen, Z., Sebastian, A., Xu, W. *et al.* (2015) Analysis of the DNA binding activities of the Arabidopsis R2R3-MYB transcription factor family by one-hybrid experiments in yeast. *PLoS ONE*, **10**, e0141044.

Kim, M.J., Jang, I.-C. and Chua, N.-H. (2016) The mediator complex MED15 subunit mediates activation of downstream lipid-related genes by the WRINKLED1 transcription factor. *Plant Physiol.* **171**, 1951–1964.

Kosma, D.K., Murmu, J., Razeq, F.M., Santos, P., Bourgault, R., Molina, I. and Rowland, O. (2014) AtMYB41 activates ectopic suberin synthesis and assembly in multiple plant species and cell types. *Plant J.* **80**, 216–229.

Kunst, L. and Samuels, L. (2009) Plant cuticles shine: advance in wax biosynthesis and export. *Curr. Opin. Plant Biol.* **12**, 721–727.

Kuraku, S., Zmasek, C.M., Nishimra, O. and Katoh, K. (2013) aLeaves facilitates on-demand exploration of metazoan gene family trees on MAFFT sequence alignment server with enhanced interactivity. *Nucleic Acids Res.* **41**, W22–8.

Lashbrooke, J., Cohen, H., Levy-Samocha, D. *et al.* (2016) MYB107 and MYB9 homologs regulate suberin deposition in Angiosperms. *Plant Cell*, **28**, 2097–2116.

Legay, S., Guerriero, G., André, C., Guignard, C., Cocco, E., Charton, S., Boutry, M., Rowland, O. and Hausman, J.-F. (2016) MdMyb93 is a regulator of suberin deposition in russeted apple fruit skins. *New Phytol.* **212**, 977–991.

Li, Y., Beisson, F., Pollard, M. and Ohlrogge, J. (2006) Oil content of *Arabidopsis* seeds: the influence of seed anatomy, light and plant-to-plant variation. *Phytochemistry*, **67**, 904–915.

Li-Beisson, Y., Shorrosh, B., Beisson, F. *et al.* (2010) Acyl-lipid metabolism. *Arabidopsis Book*, **8**, e0133.

Liu, D., Shi, L., Han, C., Yu, J., Li, D. and Zhang, Y. (2102) Validation of reference genes for gene expression studies in virus-infected *Nicotiana benthamiana* using quantitative real-time PCR. *PLoS ONE*, **7**, e46451.

Maeo, K., Tokuda, T., Ayame, A., Mitsui, N., Kawai, T., Tsukagoshi, H., Ishiguro, S. and Nakamura, K. (2009) An AP2-type transcription factor, WRINKLED1, of *Arabidopsis thaliana* binds to the AW-box sequence conserved among proximal regions of genes involved in fatty acid synthesis. *Plant J.* **60**, 476–487.

Mamode Cassim, A., Gouguet, P., Gronnier, J., Laurent, N., Germain, V., Grison, M., Boutté, Y., Gerbeau-Pissot, P., Simon-Plas, F. and Mongrand, S. (2019) Plant lipids: key players of plasma membrane organization and function. *Prog. Lipid Res.* **73**, 1–27.

Marchive, C., Nikovics, K., To, A., Lepiniec, L. and Baud, S. (2014) Transcriptional regulation of fatty acid production in higher plants: molecular bases and biotechnological outcomes. *Eur. J. Lipid Sci. Technol.* **116**, 1332–1343.

Martin, K., Kopperud, K., Chakrabarty, R., Banerjee, R., Brooks, R. and Goodin, M.M. (2009) Transient expression in *Nicotiana benthamiana* fluorescent marker lines provides enhanced definition of protein localization, movement and interactions *in planta*. *Plant J.* **59**, 150–162.

Miart, F., Desprez, T., Biot, E., Morin, H., Belcram, K., Höfte, H., Gonneau, M. and Vernhettes, S. (2014) Spatio-temporal analysis of cellulose synthesis during cell plate formation in Arabidopsis. *Plant J.* **77**, 71–84.

Molina, I., Li-Beisson, Y., Beisson, F., Ohlrogge, J.B. and Pollard, M. (2009) Identification of an Arabidopsis feruloyl-Coenzyme A transferase required for suberin synthesis. *Plant Physiol.* **151**, 1317–1328.

Nesi, N., Debeaujon, I., Jond, C., Pelletier, G., Caboche, M. and Lepiniec, L. (2000) The *TT8* gene encodes a basic helix-loop-helix domain protein required for expression of *DFR* and *BAN* genes in *Arabidopsis* siliques. *Plant Cell*, **12**, 1863–1878.

Ohlrogge, J. and Browse, J. (1995) Lipid biosynthesis. *Plant Cell*, **7**, 957–970.

Ohlrogge, J. and Jaworski, J.G. (1997) Regulation of fatty acid synthesis. *Annu. Rev. Plant Physiol. Plant Mol. Biol.* **48**, 109–136.

Oshima, Y., Shikata, M., Koyama, T., Ohtsubo, N., Mitsuda, N. and Ohme-Takagi, M. (2013) MIXTA-like transcription factors and WAX INDUCER1/SHINE1 coordinately regulate cuticle development in Arabidopsis and *Torenia fournieri*. *Plant Cell*, **25**, 1609–1624.

Paz-Arez, J. and **The REGIA Consortium** (2002) REGIA, an EU project on functional genomics of transcription factors from *Arabidopsis thaliana*. *Comp. Funct. Genom.* **3**, 102–108.

Peng, F.Y. and Weselake, R.J. (2011) Gene coexpression clusters and putative regulatory elements underlying seed storage reserve accumulation in Arabidopsis. *BMC Genom.* **12**, 286.

Pouvreau, B., Baud, S., Vernoud, V., Morin, V., Py, C., Gendrot, G., Pichon, J.-P., Rouster, J., Paul, W. and Rogowsky, P.M. (2011) Duplicate maize Wrinkled1 transcription factors activate target genes involved in seed oil biosynthesis. *Plant Physiol.* **156**, 674–686.

Prouse, M.B. and Campbell, M.M. (2012) The interaction between MYB proteins and their target DNA binding sites. *Bioch. Biophys. Acta*, **1819**, 67–77.

Prouse, M.B. and Campbell, M.M. (2013) Interactions between the R2R3-MYB transcription factor, *At*MYB61, and target DNA binding sites. *PLoS ONE*, **8**, e65132.

Punwani, J.A., Rabiger, D.S., Lloyd, A. and Drews, G.N. (2008) The *MYB98* subcircuit of the synergid gene regulatory network includes genes directly and indirectly regulated by MYB98. *Plant J.* **55**, 406–414.

Salie, M.J. and Thelen, J.J. (2016) Regulation and structure of the heteromeric acetyl-CoA carboxylase. *Biochim. Biophys. Acta*, **1861**, 1207–1213.

Salie, M.J., Zhang, N., Lancikova, V., Xu, D. and Thelen, J.J. (2016) A family of negative regulators targets the committed step of de novo fatty acid biosynthesis. *Plant Cell*, **28**, 2312–2325.

Shamloul, M., Trusa, J., Mett, V. and Yusibov, V. (2014) Optimization and utilization of *Agrobacterium*-mediated transient protein production in *Nicotiana*. *J. Vis. Exp.* **86**, 51204.

Shen, B., Allen, W.B., Zheng, P.Z., Li, C.J., Glassman, K., Ranch, J., Nubel, D. and Tarczynski, M.C. (2010) Expression of *ZmLEC1* and *ZmWRI1* increases seed oil production in maize. *Plant Physiol.* **153**, 980–987.

Solano, R., Nieto, C., Avila, J., Canas, L., Diaz, I. and Paz-Ares, J. (1995) Dual DNA binding specificity of a petal epidermis-specific MYB transcription factor (MYB.Ph3) from *Petunia hybrida*. *EMBO J.* **14**, 1773–1784.

Steffens, N.O., Galuschka, C., Schindler, M., Bülow, L. and Hehl, R. (2004) AthaMap: an online resource for *in silico* transcription factor binding sites in the *Arabidopsis thaliana* genome. *Nucleic Acids Res.* **32**, D368–272.

Tang, T., Du, C., Song, H., Aziz, U., Wang, L., Zhao, C. and Zhang, M. (2018) Genome-wide analysis reveals the evolution and structural features of WRINKLED1 in plants. *Mol. Genet. Genomics*, **294**, 329–341.

To, A., Joubès, J., Barthole, G., Lécureuil, A., Scagnelli, A., Jasinski, S., Lepiniec, L. and Baud, S. (2012) WRINKLED transcription factors orchestrate tissue-specific regulation of fatty acid biosynthesis in *Arabidopsis*. *Plant Cell*, **24**, 5007–5023.

Todd, J., Post-Beittenmiller, D. and Jaworski, J.G. (1999) *KCS1* encodes a fatty acid elongase 3-ketoacyl-CoA synthase affecting wax biosynthesis in *Arabidopsis thaliana*. *Plant J.* **17**, 119–130.

Troncoso-Ponce, M.A., Kilaru, A., Cao, X., Durrett, T.P., Fan, J., Jensen, J.K., Thrower, N.A., Pauly, M., Wilkerson, C. and Ohlrogge, J.B. (2011) Comparative deep transcriptional profiling of four developing oilseeds. *Plant J.* **68**, 1014–1027.

Troncoso-Ponce, M.A., Nikovics, K., Marchive, C., Lepiniec, L. and Baud, S. (2016) New insights on the organization and regulation of the fatty acid biosynthetic network in the model higher plant *Arabidopsis thaliana*. *Biochimie*, **120**, 3–8.

Vanhercke, T., El Tahchy, A., Shrestha, P., Zhou, X.R., Singh, S.P. and Petrie, J.B. (2013) Synergistic effect of WRI1 and DGAT1 coexpression on triacylglycerol biosynthesis in plants. *FEBS Lett.* **587**, 364–269.

Vishwanath, D.J., Kosma, D.K., Pulsifer, I.P., Scandola, S., Pascal, S., Joubès, J., Dittrich-Domergue, F., Lessire, R., Rowland, O. and Domergue, F. (2013) Suberin-associated fatty alcohols in Arabidopsis: distributions in roots and contributions to seed coat barrier properties. *Plant Physiol.* **163**, 1118–1132.

Wang, H.W., Zhang, B., Hao, Y.-J., Huang, J.H., Tian, A.-G., Liao, Y., Zhang, J.-S. and Chen, S.-Y. (2007) The soybean Dof-type transcription factor genes, *GmDof4* and *GmDof11*, enhance lipid content in the seeds of transgenic Arabidopsis plants. *Plant J.* **52**, 716–729.

Wang, Y.-M., Wang, C., Guo, H.-Y. and Wang, Y.-C. (2019) BplMYB46 from *Betula platyphylla* can form homodimers and heterodimers and is involved in salt and osmotic stresses. *Int. J. Mol. Sci.*, **20**, 1171.

Wasternack, C. (2007) Jasmonates: an update on biosynthesis, signal transduction and action in plant stress response, growth and development. *Ann. Bot.* **100**, 681–697.

Winter, D., Vinegar, B., Nahal, H., Ammar, R., Wilson, G.V. and Provart, N.J. (2007) An "electronic fluorescent pictograph" browser for exploring and analyzing large-scale biological data sets. *PLoS ONE*, **2**, e718.

Yang, W., Pollard, M., Li-Beisson, Y., Beisson, F., Feig, M. and Ohlrogge, J. (2010) A distinct type of glycerol-3-phosphate acyltransferase with sn-2 preference and phosphatase activity producing 2-monoacylglycerol. *Proc. Natl Acad. Sci. USA*, **107**, 12040–12045.

Zhong, R. and Ye, Z.-H. (2012) MYB46 and MYB83 bind to the SMRE sites and directly activate a suite of transcription factors and secondary wall biosynthetic genes. *Plant Cell Physiol.* **53**, 368–380.

Zhong, R., Lee, C. and Ye, Z.-H. (2010) Evolutionary conservation of the transcriptional network regulating secondary cell wall biosynthesis. *Trends Plant Sci.* **15**, 625–632.